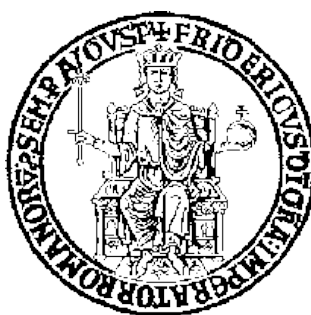


**Doctorate Program in Patology and Molecular
Fisiopatology
Doctorate School in Molecular
Medicine**

XXIV cycle - 2008–2011



**CCDC6 is a stress response protein that preserves
genome stability upon interaction with the catalytic
subunit of Serine/Threonine Protein Phosphatase 4
(PP4c)**

Coordinator:
Prof. Enrico Avvedimento

Candidate:
Chiara Luise

Supervisor:
Dr.ssa Angela Celetti

University of Naples Federico II
Dipartimento di Biologia e Patologia Cellulare e Molecolare
"L. Califano"

TABLE OF CONTENTS

ABSTRACT	4
1. INTRODUCTION.....	6
1.1 Thyroid Cancer	6
1.1.1 Classification and etiopathogenesis of thyroid carcinoma.....	6
1.2 Molecular Basis Of Well-Differentiated Thyroid Carcinoma	9
1.3 CCDC6.....	13
1.4 DNA Damage Response and cancer.....	18
1.5 Role of H2AX in genomic stability.....	20
1.6 Role of Serine/Threonine Phosphatases in the DDR.....	22
2. AIM OF THE STUDY.....	26
3. RESULTS.....	27
3.1 CCDC6 interacts with the catalytic subunit of PP4.....	27
3.2 In CCDC6 null cells the PP4c phosphatase activity is increased....	32
3.3 Loss of CCDC6 affects H2AX phosphorylation after DSBs.....	41
3.4 Loss of CCDC6 affects the DNA damage induced G2-arrest.....	47
3.5 CCDC6 loss affects DNA repair	51
4. DISCUSSION	53
5. CONCLUSIONS	57
6. MATERIALS AND METHODS	58
6.1 Materials, antibodies	58
6.2 Cell culture, plasmids and transfection.....	59
6.3 RNA interference and short hairpin mission.....	59
6.4 Western Blotting.....	60
6.5 Flow cytometry.....	61
6.6 Indirect Immunofluorescence.....	61
6.7 Chromatin extraction.....	62
6.8 Phosphatase Assays	62
6.9 G2/M checkpoint recovery assa.....	63

6.10 DSBs detection by PFGE.....	63
6.11 Clonogenic assays.....	63
7. REFERENCES.....	64
LIST OF PUBLICATIONS.....	77

ABSTRACT

This dissertation aims to understand the role of CCDC6, a gene frequently rearranged with RET in papillary thyroid carcinoma, in the signal transduction pathway activated by DNA damage. The maintenance of genomic stability is beneficial for the survival of an individual cell and crucial for cancer avoidance. Cells invest huge resources to maintain genomic stability, and cancer cells undergo an array of genetic changes to escape these barriers. The initiation of carcinogenesis represents a mutational event, which in most instances occurs despite functional DNA damage response (DDR) mechanisms. The experiments proposed in this dissertation are aimed to further investigate the mechanisms of chromosomal instability in tumor development. In particular, we will investigate the consequences of CCDC6 gene product loss or inactivation in the carcinogenetic process. CCDC6 gene product is a ubiquitously expressed 65KDa nuclear and cytosolic protein, recognised as a pro-apoptotic phosphoprotein that negatively regulates CREB1-dependent transcription. CCDC6 has been ascribed to the bona fide ATM substrates in response to genotoxic stress. Proteomic screening predicted the interaction between CCDC6 gene product and PP4c, the catalytic subunit of Protein Phosphatase 4, identified as the γ H2AX phosphatase required for recovery from the DNA damage checkpoint. We reported that, following low doses of genotoxic stress, the loss or inactivation of CCDC6, as occurs in several human cancers carrying the CCDC6 fusion proteins, increases the PP4c dependent dephosphorylation of γ H2AX, resulting in a deficient DNA damage checkpoint recovery and premature release from G2/M checkpoint arrest. Moreover, we found that the loss of CCDC6 function

affects DSBs repair. Our results indicate that CCDC6 is a stress response protein that sustains DNA damage checkpoint and contributes to genome stability maintenance in response to DNA damage by modulating PP4c activity. Overall we believe that in primary tumours the loss of CCDC6 function might contribute to the carcinogenetic process.

1. BACKGROUND

1.1 Thyroid cancer

Thyroid cancer is the most common malignancy of the endocrine organs, with an incidence of about 9-100.000 cases/year; moreover, the incidence increases with age, reaching a plateau at 50 years.

Thyroid cancer can derive from both the follicular and the parafollicular cells. More than 95% of thyroid carcinomas are derived from follicular epithelial cells, while a minority of tumours (3%), referred to as medullary thyroid carcinoma, are of C-cell origin (Figure 1).

Thyroid cancer affects women more often than men and usually occurs in people between the ages of 25 and 65 years. The incidence of this malignancy has been increasing over the last decade. Patients with a history of radiation administered in infancy and childhood for benign conditions of the head and neck, such as enlarged thymus, acne, or tonsillar or adenoidal enlargement, have an increased risk of cancer as well as other abnormalities of the thyroid gland. In this group of patients, malignancies of the thyroid gland first appear beginning as early as 5 years following radiation and may appear 20 or more years later. Other risk factors for the development of thyroid cancer include a history of goiter, family history of thyroid disease, female gender, and Asian race.

1.1.1 Classification and etiopathogenesis of thyroid carcinoma

Thyroid carcinomas are broadly divided into well-differentiated, poorly differentiated and undifferentiated types on the basis of histological and clinical parameters (Figure 1). Differentiated tumors (papillary or follicular) are highly treatable and usually curable. Poorly differentiated tumors (medullary and anaplastic) are much less common, are aggressive, metastasize early, and have a much poorer prognosis. The 10-year overall relative survival rates for patients in the United States

are 93% for papillary cancer, 85% for follicular cancer, 75% for medullary cancer, and 14% for undifferentiated/anaplastic cancer.

Papillary thyroid carcinomas (PTCs) account for around 60 to 80% of all thyroid cancers and are closely linked to ionizing irradiation (Ron et al. 1995). Young children are particularly susceptible since thyroid growth occurs primarily in childhood. A striking increase in PTC has been reported in Belarus, Ukraine and Western regions of Russia, following the Chernobyl disaster of 1986. With also a dramatic increase in the frequency of PTC in the children exposed to massive release of radionuclides (Williams 2002). PTC shows typically multicentricity and a tendency to spread into lymphatic vessels; regional node metastases at presentation are found in a significant proportion of cases. There are several PTC variants including solid-follicular, follicular, tall-cell, hurthle cell variants (Ostrowski et al. 1996). FTC is less frequent than PTC and represents about 10-30% of thyroid cancers; FTC is linked to dietary iodine deficiency (Williams et al. 1977) and shows variable morphology ranging from well-formed colloid-containing follicles, to solid or trabecular growth pattern.

Therapy for both PTC and FTC consists in surgery followed by metabolic treatment with ¹³¹I. Prognosis is very good with a survival rate at 10 years ranging from 90 to 98%. Anaplastic thyroid carcinoma (ATC) is the most aggressive type of thyroid cancer. ATC cells are extremely abnormal and spread rapidly to other parts of the body. ATC make up only about 1% of all thyroid cancers. Metastases to regional nodes are also common but their presence is often masked by the presence of extensive soft tissue invasion.

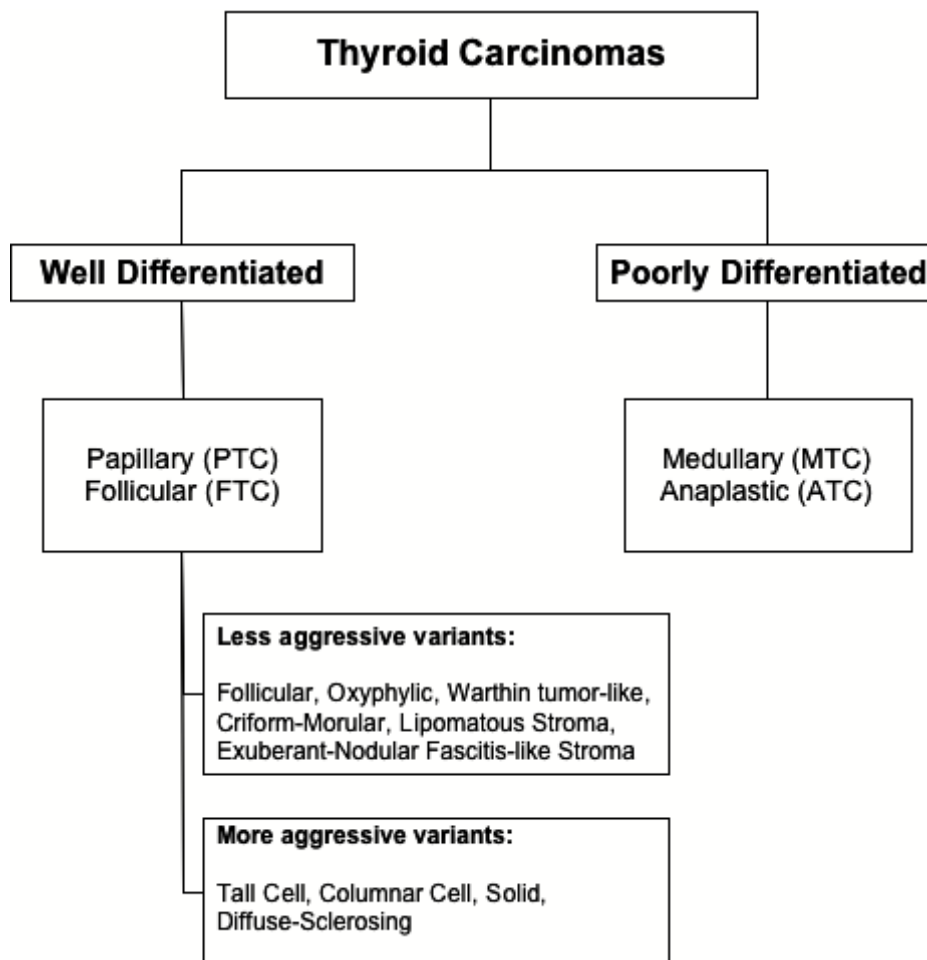


Figure 1. Classification of thyroid carcinomas. For clinical management of the patient, thyroid cancer is generally divided into 2 categories: well differentiated or poorly differentiated.

Distant metastases may be present in any site. No effective therapy is available for ATC and prognosis is extremely negative, with a mean survival of six months after diagnosis (Giuffrida et al. 2000). Finally, the medullary thyroid carcinoma (MTC) derives from the calcitonin-secreting parafollicular C cells. About 5 to 7% of all thyroid cancers are MTC; of the four types of thyroid cancers, only MTC has a clear genetic predisposition that can be passed on in families; in fact, together with pheochromocytoma, parathyroid adenoma and other tumor types, MTC

can be inherited in the context of autosomal dominant MEN 2 (multiple endocrine neoplasia type 2) syndromes (Cote et al. 2003). MEN2 syndromes are inherited cancer disorders divided in three types: MEN2A, characterized by MTC, pheochromocytoma and parathyroid adenoma; MEN2B characterized by MTC, pheochromocytoma and additional tumors such as neuromas and ganglioneuromas of the gut; Familial Medullary Thyroid Carcinoma or FMTC whose only feature is MTC. MEN2 is inherited as a highly penetrant mendelian tract and this genetic transmission is due to gain-of-function mutations of the RET gene. MTC tends to metastasize to lymph-nodes and distant organs, the treatment consists in surgical removal of the lesion. Thus, MTC are fairly resistant to most chemotherapeutic agents.

1.2 Molecular Basis of Well-Differentiated Thyroid Carcinoma

Similar to other cancer types, thyroid cancer initiation and progression occurs through gradual accumulation of various genetic and epigenetic alterations, including activating and inactivating somatic mutations, alteration in gene expression patterns, microRNA (miRNA) dysregulation and aberrant gene methylation. Thyroid cancer represents a type of neoplasia in which critical genes are frequently mutated via two distinct molecular mechanisms: point mutation or chromosomal rearrangement. In well-differentiated thyroid carcinoma non-overlapping, activating events that involve the genes RET, NTRK1 (neurotrophic tyrosine kinase receptor 1), BRAF or Ras are detectable in nearly 70% of all cases.

Papillary Thyroid carcinoma

Several studies on thyroid tumors have allowed the identification of many genetic alterations. In particular, four genetic lesions, at the somatic level, are associated with PTC. They include chromosomal aberrations targeting the RET or TRKA tyrosine kinase receptors and

point mutations in RAS or BRAF genes.

The rearranged during transfection (RET) proto-oncogene was isolated in 1985 and was the first activated receptor-tyrosine kinase to be identified in thyroid cancer (Takahashi et al 1988). The proto-oncogene, located on chromosome 10q11.2, encodes a transmembrane receptor-tyrosine kinase with four cadherin-related motifs in the extracellular domain. The exposure to ionizing radiation causes the tendency to chromosomal breaks and rearrangements with activation of oncogenes or loss-of-function suppressor genes. A frequent molecular alteration of papillary thyroid tumour is characterized by the fusion of the kinase domain of the tyrosine kinase receptor RET with the N-terminal region of constitutively expressed, heterologous genes, such as CCDC6 (RET/PTC1) or NCOA4 (RET/PTC3)(Fig. 2).

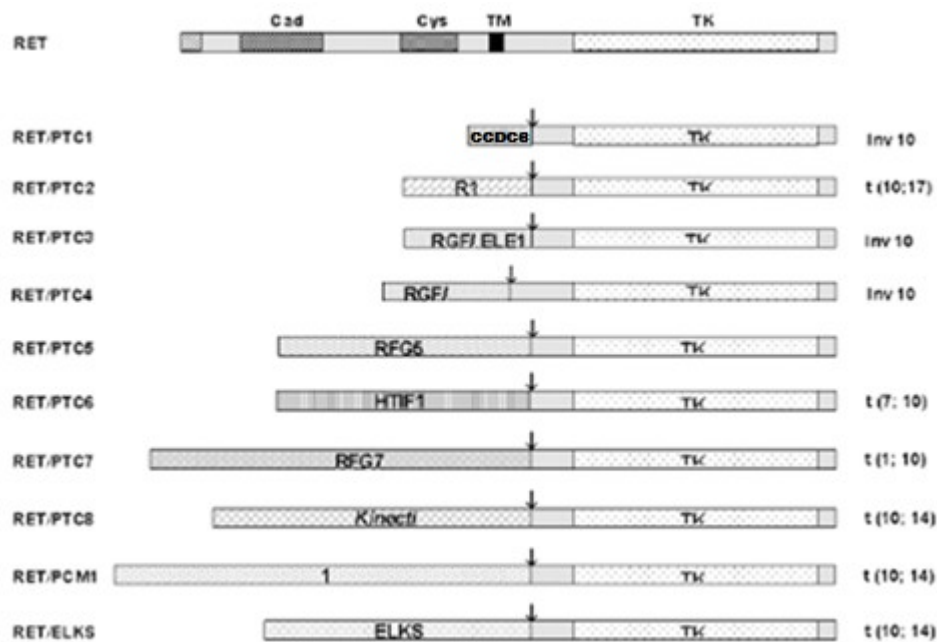


Figure 2. Chromosome 10q inversion in papillary thyroid carcinoma.

Schematic view of the paracentric inversion of chromosome 10q generating the transforming sequence RET/PTC. There are at least 10 different types of RET/PTC, all resulting from the fusion of the tyrosine kinase domain of RET to the 5' portion of different genes. RET/PTC1 and RET/PTC3 are the most common types, accounting for >90% of all rearrangements. The arrows indicate the breakpoints.

The fusion protein RET/PTC displays a constitutive activation of RET kinase function, that becomes ligand independent (Santoro et al. 1996), which leads to chronic stimulation of MAPK signaling and tumorigenesis in thyroid cells (Jhian et al., 2000; Powell et al., 1998).

More than 10 RET/PTC rearrangements have been described in sporadic and radiation-associated papillary carcinoma.

Among them the most common forms are CCDC6–RET (also known as RET/PTC1) and ELE1–RET (also known as RET/PTC3). The RET/PTC1 type of rearrangement is an inversion of chromosome 10 that mediate an illegitimate recombination between the RET and the CCDC6 genes, which are 30 megabases apart. Spatial contiguity of RET and CCDC6 within interphase nuclei may provide a structural basis for generation of RET/PTC1 rearrangement by allowing a single radiation track to produce a double-strand break in each gene at the same site in the nucleus (Nikiforova et al., 2000).

In RET/PTC1 rearrangement, the unscheduled expression of RET tyrosine kinase with its overexpression, the deletion of negative regulatory domains of the receptor and constitutive oligomerization of PTC1 proteins are responsible for PTC1-transforming activity in the thyroid. The amino terminal region of CCDC6 (paragraph 1.3) is responsible for the dimerization of the PTC1 oncoprotein in vivo. This region, containing a putative leucine zipper, mediate the dimerization and is essential for tyrosine hyperphosphorylation and the transforming activity of PTC1 (Tong et al., 1997).

Other molecular alterations are reported in papillary thyroid cancer (PTC). Point mutations in BRAF are the most common genetic lesions found, accounting for more than 45% cases of PTC (Kimura et al., 2003; Xu et al. 2003; Soares et al. 2003; Fukushima et al. 2003; Cohen et al. 2003; Nikiforov and Nikiforova 2011). BRAF, situated on 7q24, is a member of the RAF family of serine/threonine kinases and is a

component of the RAF-MEK-ERK signaling module. Activation of the RAF proteins is mediated through binding of RAS in its GTP-bound state. Once activated, RAF kinases phosphorylate MEK which in turn phosphorylates and activates ERK (Malumbres et al. 2003). A Glutamine for Valine substitution at residue 600 (V600E) in the activation segment accounts for more than 90% mutations of BRAF in PTC (Kimura et al. 2003; Cohen et al. 2003; Soares et al. 2003; Salvatore G. 2006). This mutation enhances BRAF activity through disruption of the autoinhibited state of the kinase. BRAF mutations in papillary thyroid carcinoma correlate with distant metastasis and more advanced clinical stage, and occur at a significantly higher frequency in older patients.

The neurotrophic receptor-tyrosine kinase NTRK1 (also known as TRK and TRKA) was the second identified subject of chromosomal rearrangement in thyroid tumorigenesis. The NTRK1 proto-oncogene (which is located on chromosome 1q22) encodes the transmembrane tyrosine-kinase receptor for nerve growth factor. The activated receptor initiates several signal-transduction cascades, including ERK, PI3K and the phospholipase-Cgamma (PLCgamma) pathways. NTRK1 rearrangements, known as TRK rearrangements, which show ectopic expression and constitutive activation of the tyrosine kinase analogous to RET rearrangements, have been noted in 5–13% of sporadic tumors but only in 3% of post-Chernobyl childhood papillary thyroid carcinomas. Unlike other solid neoplasms, Ras is the least prominent participant in thyroid carcinogenesis. Three Ras proto-oncogenes are implicated in human tumorigenesis: HRAS (which is located on chromosome 11p11), KRAS (which is located on chromosome 12p12), and NRAS (which is located on chromosome 1p13). Mutations involving codon 61 of HRAS and NRAS have been reported with variable frequency in thyroid neoplasms (Rivera et al., 2010). Ras mutations are more common in iodine-deficient than iodine-sufficient areas and mostly found in lesions

with follicular architecture (including follicular carcinoma and follicular variant papillary thyroid carcinoma) rather than in typical papillary thyroid carcinoma. Interestingly, activating Ras mutations are rare in radiation-induced thyroid cancers of Chernobyl. Notably in human papillary thyroid cancer, the genetic alterations of RET/PTC, RAS and BRAF are mutually exclusive, suggesting the existence of a common signaling cascade; moreover, mutations at more than one of these sites are unlikely to provide an additional biological advantage (Kimura et al. 2003, Cohen et al. 2003, Soares et al. 2003, Nikiforov and Nikiforova 2011).

1.3 CCDC6

The CCDC6 gene (Coiled Coil Containig 6) has been identified upon its frequent rearrangement with the RET proto-oncogene in papillary thyroid carcinomas. The CCDC6 gene, also called H4(D10S170), maps on the long arm of chromosome 10 at 10q21 (Grieco et al. 1990), and contains 9 exons that encode for a transcript of 3 Kb and shows an open reading frame (ORF) of 585 aa. The CCDC6 gene promoter, localized within 259 bp upstream of the ATG site, drives the gene expression ubiquitously in various human tissues including thyroid (Tong et al. 1995). Since the CCDC6 gene is ubiquitously expressed, the specificity of the PTC-1 activation is due to the specificity for thyroid tissue of the somatic rearrangement of the *ret* proto-oncogene. In thyroid tumours harbouring the RET/PTC1 rearrangement, activation of RET involves chromosomal inversion of the long arm of chromosome 10 that juxtaposes the tyrosine kinase-encoding domain of RET mapped at 10q11.2 to the promoter and the first exon of a new gene, CCDC6 gene, mapped at 10q21 (Pierotti et al., 1992) (Fig.3). Cloning and sequencing of CCDC6 cDNA did not show any significant homology to known genes. Its predicted amino-acid (aa) sequence

contains a long coiled-coil region and a putative binding domain for SH3-proteins, suggesting its possible involvement in protein–protein interactions (Grieco et al., 1994). SH3-binding domains play an important role in protein-protein interactions in numerous cellular processes. The presence of a putative SH3-binding domain in CCDC6 gene product suggests that this protein might be a cytoskeletal one. Sequence analysis of CCDC6 gene product shows extensive regions of alpha helices which have a high potential to adopt a coiled-coil conformation. Coiled-coils are formed by two or three alpha-helices that are strongly amphipathic and supercoil around each other, crossing at an angle of ca 20° (Lupas et al 1991). It has been shown that such regions can be involved in protein dimerization or oligomerization. The 60 amino acid fragment of the CCDC6 coiled-coil domain included in the RET/PTC1 product, has been shown to be necessary for homo-dimerization, constitutive activation and transforming ability of the oncoprotein (Tong et al., 1997; Jhiang, 2000).

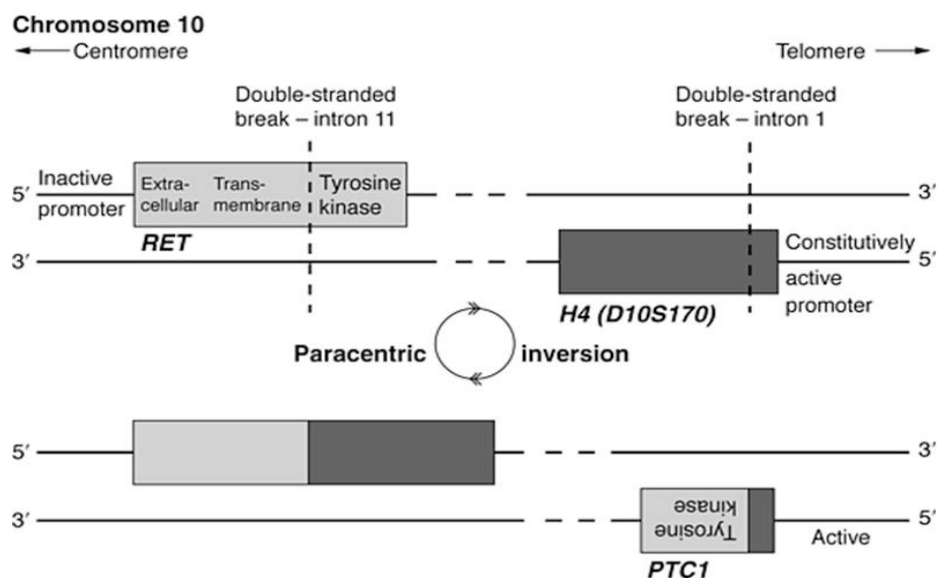


Figure 3. Schematic view of the paracentric inversion of chromosome 10q generating the transforming sequence RET/PTC1.

It is not clear why RET/PTC1 has been found activated only in thyroid papillary carcinomas, since in vitro irradiation is able to induce its activation also in fibroblasts (Ito et al. 1993).

Nikiforova et al. (2000) suggested that the spatial contiguity of RET and CCDC6 chromosomal loci might be responsible for the high frequency of RET/PTC1 radiation induced rearrangements in thyroid human cells.

The CCDC6/RET rearrangement is not the only one involving the CCDC6 gene, although it is the more frequent.

A new chromosomal rearrangement involving the CCDC6 gene has been recently described (Fig.4), suggesting that CCDC6 gene has high susceptibility for recombination. In two cases of atypical chronic myelogenous leukaemia (CML), the first 368 aa of CCDC6 fuse to the PDGF β R tyrosine kinase domain. The chromosomal event is a t(5;10) translocation. In the two cases of atypical CML in which the CCDC6-PDGF β R transcript has been identified, the fusion gene codes for a 948 aa protein with most of the coiled-coil of CCDC6 and the transmembrane and the tyrosine kinase domains of the PDGF β R. The fusion protein oligomerization and constitutive activity is dependent on the coiled-coil domain of the CCDC6 gene. The reciprocal product of the translocation has not been found (Kulkarni et al., 2000; Schwaller et al., 2001). Moreover, more recently, it has been reported the characterization of a new chromosome 10 rearrangement involving CCDC6 and PTEN genes. The CCDC6/PTEN rearrangement was discovered in irradiated thyroid cell lines. Sequencing revealed a transcript consisting of exon 1 and 2 of CCDC6 fused with exons 3-6 of PTEN.

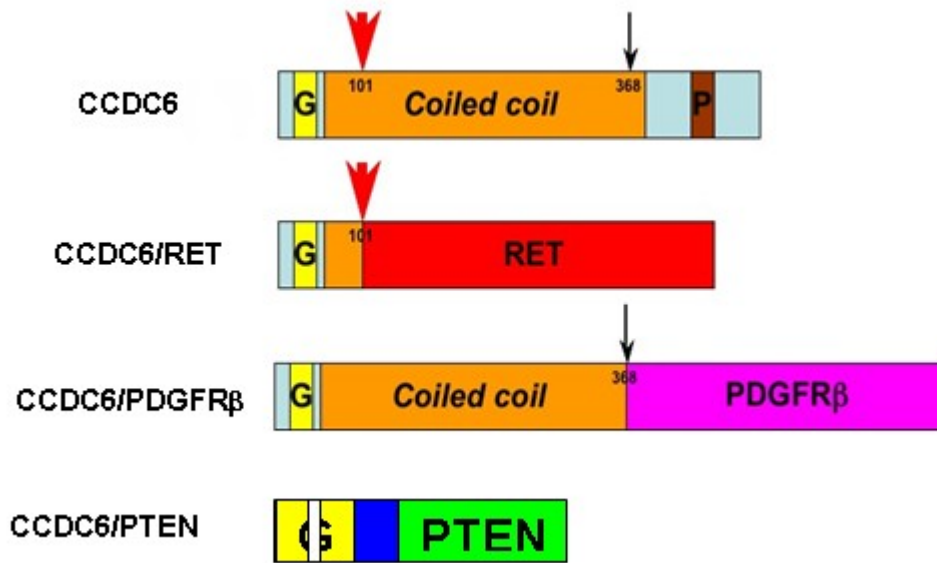


Figure 4 CCDC6 rearrangements. The red arrow shows the RET/PTC1 and the black one shows the CCDC6/PDGFBetaR and CCDC6/PTEN breakpoints.

The disruption of the normal regulation of the RET kinase is critical to the transforming properties, less is known about whether disruption of the normal function of the 5' partner gene might also have an important role. To address this point, the identification of the normal physiological function of the heterologous RET fusion partners is required. During the last years it has been characterized the product of the first and most frequently observed RET-fused gene, CCDC6.

CCDC6 gene product has been described as a ubiquitously expressed 65KDa nuclear and cytosolic protein with no significant homology to known genes. In the last few years, several large-scale phosphorylation site-mapping studies recognized CCDC6 as a phosphoprotein (Beausoleil *et al.*, 2004; Brill *et al.*, 2004). Nevertheless, previous investigations reported that CCDC6 is phosphorylated by ERK1/2 at serine 244 upon serum induction (Grieco *et al.*, 1994; Celetti *et al.*, 2004). CCDC6 wild type induces the apoptosis and its truncated mutant 1-101, that correspond to the portion of CCDC6 included in RET/PTC1, acts as dominant negative on nuclear localization and on the wild-type

protein-induced apoptosis (Celetti *et al.*, 2004). Furthermore, CCDC6 protein is involved in ATM-mediated cellular response to DNA damage. The kinase ataxia telangectasia mutated (ATM) phosphorylates a limited number of downstream protein targets in response to DNA damage. The potential role of CCDC6 in DNA damage signaling pathways has been investigated and it has been reported that in cells treated with etoposide or ionizing radiation (IR), CCDC6 underwent ATM-mediated phosphorylation at Thr 434, stabilizing nuclear CCDC6. The expression of CCDC6 with threonine 434 mutated in Alanine, CCDC6T434A, protected the cells from genotoxic stress-induced apoptosis. Most importantly, after exposure to IR silencing of CCDC6 in mammalian cells increased cell survival, allows for DNA synthesis and permits cells to progress into mitosis (Merolla *et al.*, 2007).

These data suggest that impairment of CCDC6 gene function might have a role in thyroid carcinogenesis. Further supporting a role in the control of proliferation, it has been recently demonstrated that CCDC6 interacts and inhibits CREB1-dependent transcription (Leone *et al.*, 2010). Thus, it is possible to postulate that the transforming potential of RET/PTC1 is not confined to the RET tyrosine kinase activation, but it may also involve the disruption of the CCDC6 gene product. In this way CCDC6 has been proposed as a new tumor suppressor. Finally, we reported the identification and characterization of three sites of sumoylation in CCDC6, (K74, K266 and K424), highly conserved in vertebrates. We demonstrated that CCDC6 is sumoylated on these sites mainly by SUMO2. The post-translational modifications by SUMO constrain most of the CCDC6 protein in the cytosol and affect its functional interaction with CREB1. Sumo modifications, loosing the CCDC6-CREB1 interaction, lead to a decrease of CCDC6 repressive function on CREB1 transcriptional activity. Interestingly, in thyroid cells the SUMO2-mediated CCDC6 post-translational modifications are

amplified by forskolin, a cAMP analog. Thus, CCDC6 could be an important player in the dynamics of cAMP signaling, fine regulating CREB1 transcriptional activity in normal and transformed thyroid cells (Luise C. et al., submitted).

1.4 DNA damage response and cancer

Maintenance of genomic integrity is an essential part of cellular physiology. Genotoxic insults that induce DNA breaks must be repaired in order to prevent the mutations that can contribute to malignant transformation. The processes by which cells repair damage to DNA and coordinate repair with cell cycle progression are collectively known as the DNA damage response (DDR).

In cases in which the damage cannot be repaired, prolonged cell cycle arrest can lead to senescence or the induction of apoptotic signals (Zhou BB et al., 2000; Norbury CJ, Zhivotovsky B., 2004). During cancer progression the ATM, ATR, DNA-PK Ser/Thr Kinases mediate DNA damage-induced signal transduction and are often mutated (Motoyama and Naka, 2004). DNA damage is recognized by sensor proteins that initiate the activation of the DDR on chromatin. These sensors include the Mre11-Rad50-Nbs1 (MRN) and the Rad9-Rad1-Hus1 (9-1-1) complexes that localize to double stranded breaks (DSBs) or regions of replication stress and single stranded breaks, respectively (Lee JH et al., 2007) (Fig.5). Mre11 binds to Nbs1, DNA, and Rad50 and possesses DNA exonuclease, endonuclease, and unwinding activities. While Rad50 may function to keep the broken ends of the DNA together, Nbs1 functions to recruit signal transducing kinases to the break site and mediates the DDR signal (Alyson K Freeman, Alvaro NA Monteiro 2010).

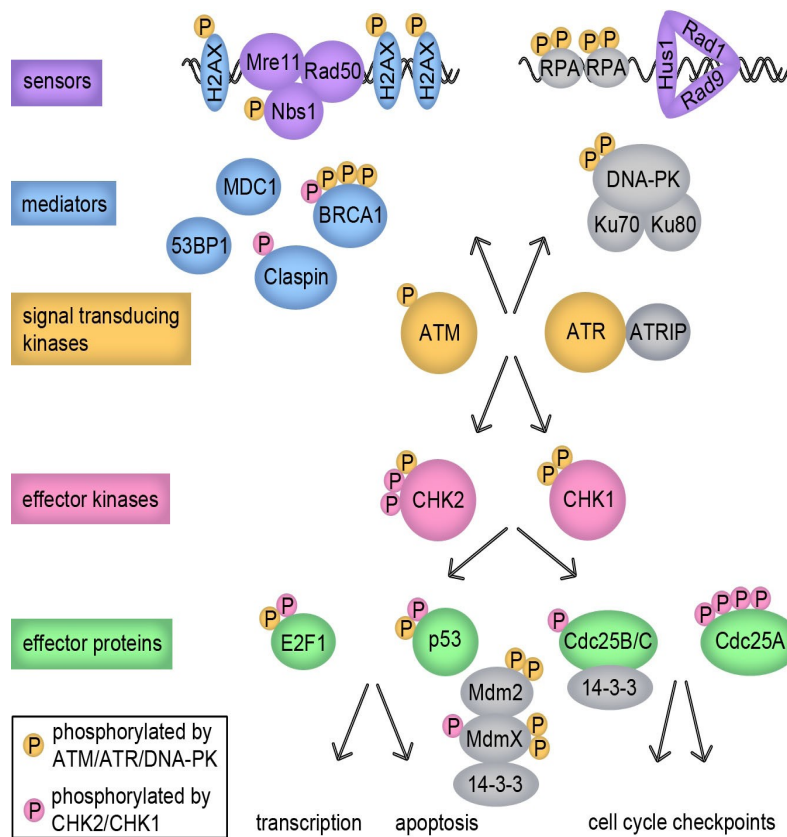


Fig 5: A simplified view of the cellular response to DNA damage. Single and double stranded DNA breaks signal through the sensors (MRN and 9-1-1) shown in purple, mediators (H2AX, BRCA1, MDC1, 53BP1) shown in blue, signal transducing kinases (ATM, ATR) shown in yellow, effector kinases (CHK2, CHK1) shown in pink, and effector proteins (E2F1, p53, Cdc25) shown in green, leading to gene transcription, apoptosis, and cell cycle arrest. Proteins that are phosphorylated by ATM, ATR, and/or DNA-PK are marked by a yellow phosphate group and proteins that are phosphorylated by CHK2 and/or CHK1 are marked by a pink phosphate group.

The localization of the MRN and 9-1-1 complexes to the sites of DNA damage in chromatin signals to activate the signal transducing kinases Ataxia-telangiectasia mutated (ATM), the ATM and Rad3-related (ATR) kinase, and the DNA-dependent protein kinase (DNAPK), which are members of the phosphoinositide 3-kinase related kinase family. The first event in response to DSB is a ATM autophosphorylation at S1981,

that caused dissociation from inactive dimers into active monomers (Bakkenist CJ, Kastan MB, 2003). The second event: ATM phosphorylates Nbs1 on S343 and at the same time, Nbs1 and the MRN complex are required for full activation of ATM. The localization of ATR to the break site and its subsequent activation is dependent upon the 9-1-1 complex, binding between ATR and ATR-interacting protein (ATRIP), and replication protein A (RPA). The signal transducing kinases ATM and ATR signal through the effector kinases CHK1 and CHK2 (checkpoint kinase 1 and checkpoint kinase 2). CHK2 is activated primarily in response to DSB through the phosphorylation of T68 by ATM and subsequent oligomerization and autophosphorylation at T383 and T387. CHK1 is active even in unperturbed cells, but is further activated through the phosphorylation of S317 and S345 by ATR, primarily in response to single stranded breaks and replication stress (Bartek J, Lukas J, 2003). Several mediator proteins such as BRCA1, MDC1, Claspin, 53BP1 and H2AX, work to coordinate the localization of various factors in the DDR, promote their activation, and regulate substrate accessibility. BRCA1 S1387 and S1423 are targets of phosphorylation by ATM and these phosphorylations are required for the intra-S and G2/M checkpoints, respectively. MDC1 functions as a molecular scaffold to mediate parts of the DDR downstream of foci formation (Mohammad DH, Yaffe MB, 2009). Claspin is a major regulator of the activity of CHK1 and binds DNA with high affinity (Kumagai A, Dunphy WG 2000; Chini CC, Chen J 2006). H2AX is phosphorylated by ATM, ATR and DNA-PK on S139 upon DNA damage and this phosphorylated form is also known as γ -H2AX.

1.5 Role of H2AX in genomic stability

Genomic instability is generally used to describe a genetic predisposition for an increase in chromosomal pathology secondary to

inaccurate repair or deficiency in cell cycle checkpoints. Typically, the instability can be visualized as chromosomal breaks, translocations, or aneuploidy.

DNA damage occurs following a variety of stimuli including ionizing radiation (IR), ultraviolet radiation (UV), replication stress, chemicals from the environment, and reactive oxygen species that are produced as a byproduct of cellular metabolism (Alyson K Freeman, Alvaro NA Monteiro 2010).

Among all types of DNA damage, double strand breaks (DSBs) are believed to be the most dangerous. DSBs occur naturally during V(D)J recombination and meiosis, and can be induced by oxidative stress, radiation or genotoxic chemicals. DSBs present a major threat to genomic integrity by promoting chromosomal instability, ultimately leading to cancer. The cellular genomic integrity is monitored by processes that detect and repair DSBs and that also halt cell cycle progression until repair is complete. Human diseases with defects in these processes often exhibit a predisposition towards cancer.

A key component in the maintenance of genomic stability is the protein H2AX, which is a member of the histone H2A family, one of the five families of histones that package and organize eukaryotic DNA into chromatin. The phosphorylation of H2AX is among the earliest responses to DNA damage, and controls the widespread accumulation of checkpoint response proteins to large chromatin regions surrounding the break sites (Rogakou *et al.*, 1998). Within minutes following exposure to ionizing radiation (IR), activated ATM phosphorylates H2AX in the C-terminal tail at Ser139 over a region of megabases surrounding a DSB (Burma *et al.* 2001). In a parallel manner, ATR phosphorylates H2AX after replicational stress (Ward and Chen 2001). The phosphorylation of H2AX is induced in response to DSBs originating from diverse origins including external damage, replication fork collision,

apoptosis, and dysfunctional telomeres.

The recruitment of DNA damage signaling and repair proteins to sites of genomic damage constitutes a primary event triggered by DNA damage. Many components of the DNA damage response, including ATM, BRCA1, 53BP1, MDC1, RAD51, and the MRE11/RAD50/NBS1 (MRN) complex form ionizing radiation induced foci (IRIF) that co-localize with γ -H2AX foci.

To cope with genotoxic damage, cells activate powerful DNA damage-induced cell cycle checkpoints that coordinate cell cycle arrest with recruitment and activation of the DNA repair machinery (Bartek and Lukas, 2007; Harper and Elledge, 2007; Kastan and Bartek, 2004; Shiloh, 2003; Zhou and Elledge, 2000). The overall importance of these cell cycle checkpoints in maintaining genomic integrity is highlighted by the observation that the loss, mutation, or epigenetic silencing of checkpoint genes is frequently observed in cancer (Hoeijmakers, 2001). Dephosphorylation of γ H2AX (the phosphorylated form of H2AX on Ser 139) and its exclusion from chromatin regions distal to the break sites are crucial to resume the cell cycle (Fernandez-Capetillo *et al.*, 2004). In this way, the phosphorylation status of H2AX constitutes a molecular switch that helps to maintain genomic integrity.

1.6 Role of Serine/threonine phosphatases in the DDR

The fine-tuning of response to damage depends on the activity of phosphatases in order to prevent illegitimate activation of the DDR in the absence of damage and to allow rapid cessation of the signal once DNA is repaired. Ser/Thr phosphatases are known regulators of a variety of cellular processes: gene transcription, RNA splicing, DNA replication; moreover phosphatases may also be involved in cancer progression. (Moorhead *et al.*, 2007; Virshup and Shenolikar, 2009; Peng A & Maller JL, 2010). Ser/Thr protein phosphatases (PP) have been classified

biochemically into type 1 (PP1) and type 2 (PP2). In humans, PP1 contains three isoforms (α , β and γ), each encoded by a distinct, but related, gene. PP2 is divided into three groups on the basis of metal-dependence: metal-independent PP2A, PP4, PP5 and PP6; Ca^{++} -dependent PP2B and PP7; and $\text{Mg}^{+}/\text{Mn}^{+}$ -dependent PP2C. PP2C is highly conserved and encoded by seven genes in *Saccharomyces cerevisiae* and 16 genes in humans. Family members of PP2C are essential regulators of various cellular processes, including stress signaling, cell differentiation, growth, apoptosis and others (Lu and Wang, 2008). Several groups of Ser/Thr phosphatases, particularly PP2C δ /Wip1, PP2A and PP1, have been linked to DDR regulation (Heideker et al., 2007).

PP2A removes γ -H2AX foci formed in mammalian cells, in response to DNA damage by the topoisomerase I inhibitor camptothecin (CPT) (Chowdhury et al., 2005). PP2A δ colocalizes at γ -H2AX foci, suggesting that PP2A dephosphorylates γ -H2AX near a DSB.

PP6, another PP2A-like phosphatase, has also been implicated in γ -H2AX dephosphorylation mediated by regulatory subunits PP6R1, PP6R2 or PP6R3 (Douglas et al., 2010).

Recently, it has been suggested that Wip1 also participates in γ -H2AX dephosphorylation after DNA damage (Cha et al., 2010; Macurek et al., 2010; Moon et al., 2010).

Indeed γ -H2AX is regulated by multiple phosphatase (Fig.6).

Previously, a study in yeast identified Pph3, the orthologue of mammalian PP4, as a key element of checkpoint recovery that dephosphorylates γ -H2AX (Keogh et al., 2006), in response to DNA damage by irradiation or chemical mutagens. Keogh et al. found that a complex (HTP-C) containing the Pph3 phosphatase enzyme specifically regulated the dephosphorylation of γ -H2AX, an event that is crucial for release from the damage checkpoint.

Mammalian Ppp4c was predicted from different cDNAs and its 65% amino acid identity to PP2Ac α and PP2Ac β isoforms and extremely high conservation to *D. melanogaster* (94% amino acid identity) suggested that it was likely to have distinct cellular roles from PP2A (Helps et al., 1998; Brewis, N.D. and Cohen, P.T.W., 1993; da Cruz e Silva, 1988).

Protein phosphatase 4 (Ppp4/PP4/PPX) is a ubiquitous protein phosphatase that removes phosphates from serine and threonine in proteins and regulates many cellular functions independently of other related protein phosphatases in the PPP family (Cohen, P.T.W., 2004).

PP4c has been implicated in TNF α signaling (Mihindukulasuriya et al., 2004; Zhou et al., 2002) and NF- κ B regulation (Hu et al., 1998; Yeh et al., 2004). Recently, histone deacetylase 3 (HDAC3) and a mitotic regulatory protein NDEL1 were shown to be regulated by a specific PP4 complex (Chowdhury et al., 2008). Protein Phosphatase 4 is structurally and functionally related to PP2A and follows the same general rules for assembly and regulation. PP4, like PP2A, forms obligate heterodimers and heterotrimers (Chen et al., 2008). At least six regulatory subunits of PP4 have been identified. Both PP2A and PP4 dephosphorylate the phosphorylated histone 2A variant, γ -H2AX, a marker for DNA damage and cell-cycle arrest. However, each phosphatase plays a different physiological role, with PP2A functioning after DNA damage and PP4 at site of chromatin breakage (Chowdhury et al., 2005). Mammalian PP4 is the functionally important γ -H2AX phosphatase during S phase. A specific PP4 heterotrimeric complex containing the catalytic subunit (PP4C), the scaffolding subunit PP4R2, and the targeting subunit, PP4R3 β , returns H2AX to its fully dephosphorylated state during DNA replication and in response to genotoxic stress (Chowdhury et al., 2008; Nakada et al., 2008). Moreover, a PP4 phosphatase complex dephosphorylates RPA2 to facilitate DNA repair via homologous recombination in response to DSBs (Lee D-H, 2010).

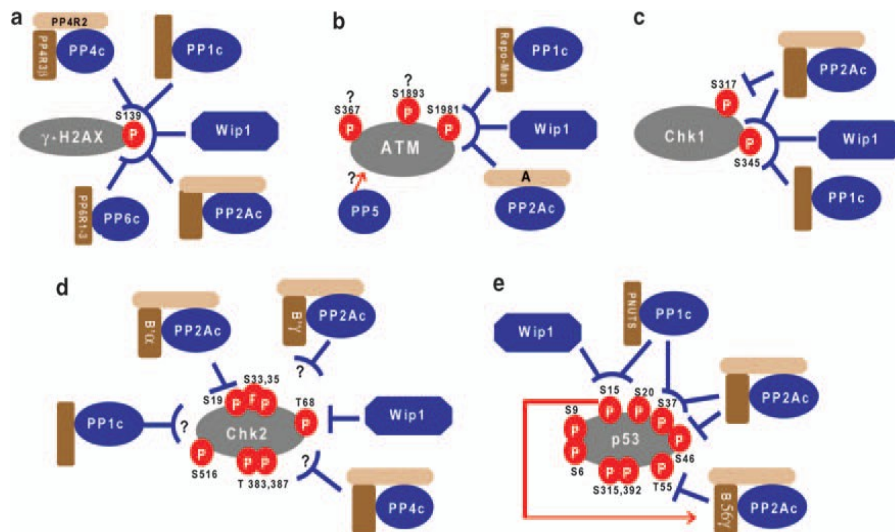


Fig.6 Phosphorylation of key DDR factors is specifically controlled by Ser/Thr phosphatases.

(a) γ -H2AX has been reported to be dephosphorylated at Ser 139 under various conditions by PP1, PP2A, PP4, PP6 and Wip1. (b) ATM is dephosphorylated at Ser 1981 by PP1, PP2A and Wip1. It is unclear whether Ser 367 and 1893 are also targeted by these phosphatases or how PP5 promotes ATM activation (as denoted by question marks). (c) Wip1 dephosphorylates Chk1 at Ser 345, PP2A dephosphorylates Chk1 at both Ser 345 and 317 and the PP1 homolog in yeast dephosphorylates Chk1 at Ser 345. (d) PP2A/B0a and Wip1 dephosphorylate Chk2 at Ser 19 and Ser 68, respectively. PP2A/B0g dephosphorylates and deactivates Chk2, as judged by its electrophoretic mobility and kinase activity. Yeast homologs of PP4 and PP1 regulate yeast Chk2 at undefined sites (as denoted by question marks). (e) Wip1 dephosphorylates p53 at Ser 15, a phosphorylation site that recruits PP2A/B56g to p53 to dephosphorylate Thr 55. PP1/PNUTS dephosphorylates p53 at Ser 15 and 37. PP2A does not regulate p53 phosphorylation at Ser 15, but can dephosphorylate p53 at Ser 37 and 46.

2. AIM OF THE STUDY

The experiments proposed in this dissertation are aimed to further investigate the mechanisms of chromosomal instability in tumor development. In particular, we will investigate the consequences of CCDC6 gene product loss or inactivation as we hypothesize that CCDC6 loss in tumours might elicit the carcinogenetic process contributing to genomic instability. Recent high-throughput proteomic screening predicted the interaction between CCDC6 gene product and the catalytic subunit of PP4 (PP4c), recently identified as the γ H2AX phosphatase required for recovery from DNA damage checkpoint.

The purpose of the present investigation is then to verify:

1. if CCDC6 interacts with the catalytic subunit of Protein Phosphatase 4;
2. the minimal region of interaction between CCDC6 and PP4c;
3. The relationship between CCDC6 and the regulatory subunits of PP4c, and in particular whether:
 - CCDC6 is necessary for the assembly of the holoenzyme PP4
 - the interaction between CCDC6 and PP4c is direct or mediated by other regulatory subunits;
4. the enzymatic activity of PP4c upon DNA damage in CCDC6 null cells;
5. the phosphorylation status of H2AX upon DSBs in CCDC6 null cells;
6. the DNA damage induced G2 arrest and checkpoint recovery in CCDC6 null cells;
7. the DNA repair upon DSBs in CCDC6 null cells.

3. RESULTS

3.1 CCDC6 interacts with the catalytic subunit of PP4

The interaction of protein phosphatase PP4c and CCDC6 has been reported, but the significance of this interaction has not been investigated yet (Chen *et al.*, 2008; Ewing *et al.*, 2007). The catalytic subunit of PP4 (PP4c), a member of PPP serin-threonin-phosphatase family, has been implicated in microtubule organization at centrosome, in DNA-damage response and recently in dephosphorylation of γ H2AX, a key DNA-repair protein (Cohen *et al.*, 2005; Nakada *et al.*, 2008; Chowdhury *et al.*, 2008).

To aid in the characterization of the reported interaction, we transfected 293T cells with a myc-tagged CCDC6 wt and two truncated mutants of 223 and 101 aa length (CCDC6 1-223; and CCDC6 1-101). Co-precipitation of PP4c was detected only with the myc-CCDC6 wt protein, and not with the truncated mutants, by immunoblotting with specific anti-myc antibodies (Figure 9), indicating that the interaction occurs at the carboxy-terminus of CCDC6 gene product.

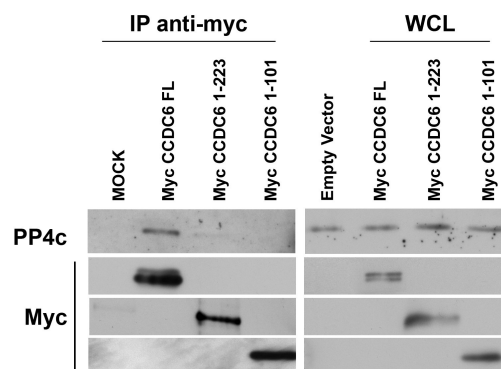


Fig.9 CCDC6 interacts with PP4c

293T cells were transfected with CCDC6 or the CCDC6 (1-223) and (1-101) deleted mutant constructs. Whole cell lysates (WCL) were prepared and equal amounts of

proteins were immunoprecipitated with anti Myc. Then, the immunocomplexes were analyzed by western blotting using the indicated antibodies. Mock indicates negative control of immunoprecipitation using an unrelated antibody

Indeed, RET/PTC1 oncoprotein, including the first 101 aa of CCDC6 fused to RET tyrosine kinase, was unable to interact with PP4c (Figure 10).

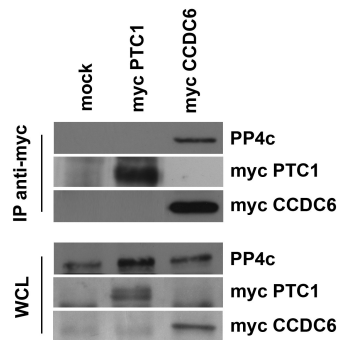


Fig.10

293T cells were transfected with CCDC6wt or the PTC1 constructs. Whole cell lysates (WCL) were prepared and equal amounts of proteins were immunoprecipitated with anti-myc. Then, the immunocomplexes were analyzed by western blotting using anti-PP4C and anti-myc antibodies. Mock indicates negative control of immunoprecipitation using an unrelated antibody.

We assessed whether endogenous PP4c could co-immunoprecipitate CCDC6 at endogenous level. Immunoblotting for CCDC6 revealed the co-precipitation of a doublet at the expected size in HeLa cells (Figure 11). Importantly, endogenous CCDC6 immunoprecipitated endogenous PP4c and we found that this interaction is specific as CCDC6 does not co-immunoprecipitate with the endogenous protein phosphatase PP2A, PP6 and Wip1 as phosphatases reported to be involved in regulation of γ H2AX in context of DNA damage and checkpoint recovery (Figure 12).

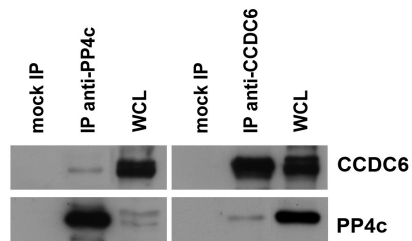


Fig.11 The co-immunoprecipitation was performed on the endogenous CCDC6 and PP4c proteins obtained from parental 293T cells. The immunocomplexes were analyzed by western blotting using the indicated antibodies.

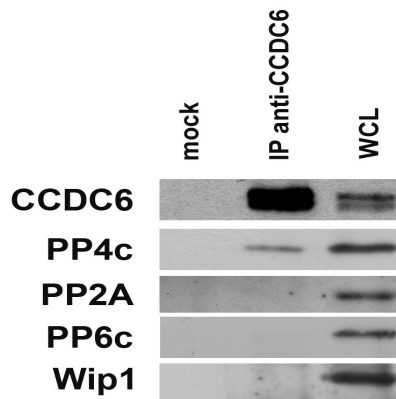


Fig.12 The co-immunoprecipitation was performed on the endogenous CCDC6 and the immunocomplexes were analyzed by western blotting using PP4c, PP2A, PP6c and Wip1 antibodies.

To further understand the PP4c-CCDC6 interaction, we mapped the region within CCDC6 that is required for this interaction. We tested two truncated forms of CCDC6 at the C-terminal domain, the CCDC6 (aa. 139-474) and the CCDC6 (aa. 410- 474) both including the proline-rich

region. As shown by the GST-pull down experiments, we found that in CCDC6 the minimal region of interaction with PP4c is confined to the Proline-Rich stretch (aa 410-474), as predicted and also reported for other PP4c interacting proteins, such as Hpk1 (Zhou *et al.*, 2004) (Figure 13).

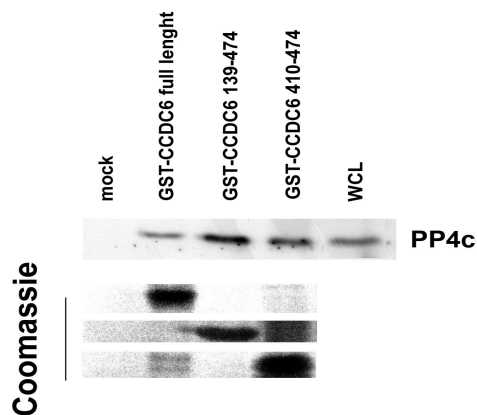


Fig.13 GST pull-down assays were performed on WCL from 293T cells and the GST (mock) or GST-CCDC6 fusion proteins. The bound complexes and WCL were separated on SDS-PAGE and analyzed by western blotting with the indicated antibodies. Coomassie staining is shown as loading control.

PP4 is a protein complex conserved from yeast to human cells and contains in addition to PP4c, the PP4R2 and PP4R3 regulatory subunits (Chowdhury *et al.*, 2008; Nakada *et al.*, 2008).

In order to understand if the PP4 regulatory subunits mediate the interaction between PP4c and CCDC6 we silenced the subunits R2, R3 α and R3 β and we found that their depletion did not affect the interaction between CCDC6 and PP4c (Figure 14, 15). The silencing of PP4R1 and PP4R4 did not affect their interaction, too (Figure 16, 17). Notably, CCDC6 was able to co-immunoprecipitate with R2, R3 α and R3 β , but not with R1 and R4, at least in our experimental conditions (Figure 14, 15, 16 and 17).

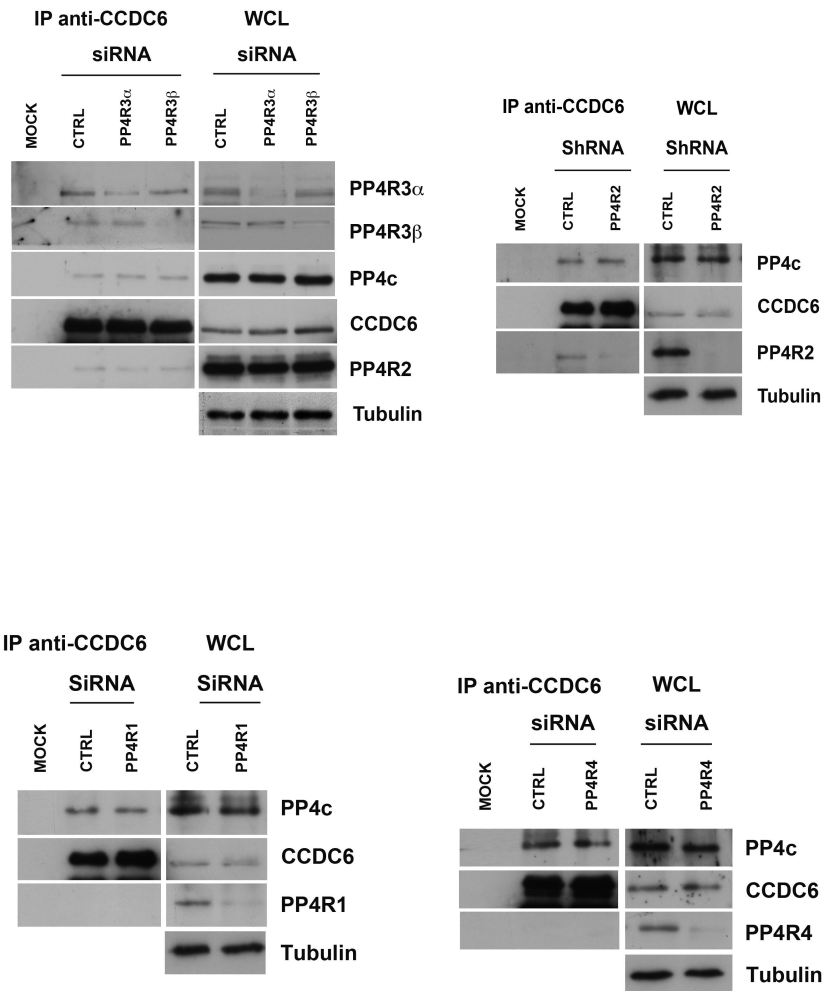


Fig.14-15-16-17 In 293T cells, siRNAs targeting specific PP4 regulatory subunits reduced their expression as shown; coimmunoprecipitations were performed on the endogenous CCDC6 and the immunocomplexes were analysed by western Blot using several antibodies, as indicated. Mock indicates negative control of immunoprecipitation using an unrelated antibody. Tubulin show the loading control.

3.2 In CCDC6 null cells the PP4c phosphatase activity is increased

We previously reported that CCDC6 is involved in the ATM-mediated cellular response to DNA Damage (Merolla et al., 2007). In order to evaluate the functional outcome of the interaction between CCDC6 and PP4c, we investigated if CCDC6 could modulate the enzymatic activity of the phosphatase on one of its known substrate, the phospho-Histone H2AX. As a source of phosphatase, we immunopurified endogenous PP4c to retain as much as possible of the subunits composition of PP4 holoenzyme complexes (Tung *et al.*, 1985; Nakada *et al.*, 2008; Macurek et al, 2010).

In CCDC6-depleted HeLa cells (shCCDC6), compared to control cells (shCTRL), the endogenous immunopurified PP4 complex showed increased activity on phospho-H2AX-enriched chromatin, obtained, from cells exposed to DNA damage, by cells-fractionation and tested for γ H2AX expression (Figure 18a).

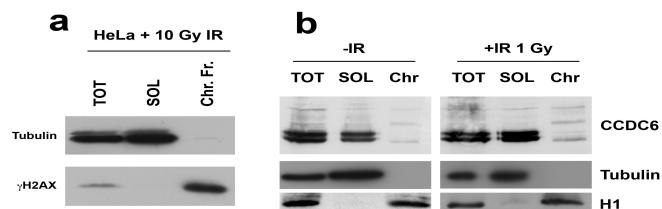


Fig.18a-b Chromatin fractions were purified by HeLa cells after 10 Gy IR exposure, as reported in Supplementary experimental procedures. Enriched phosphorylated H2AX is shown in the chromatin fraction. The anti CCDC6 hybridization shows that a quote of CCDC6 is also localized on chromatin

The phosphatase reactions were followed by immunoblotting and probed with the specific antibodies as shown in Figure 19. Immunopurified PP4R2, R3 α and R3 β were also revealed at IB, in PP4c

immunoprecipitates, inferring that the protein complex might be active.

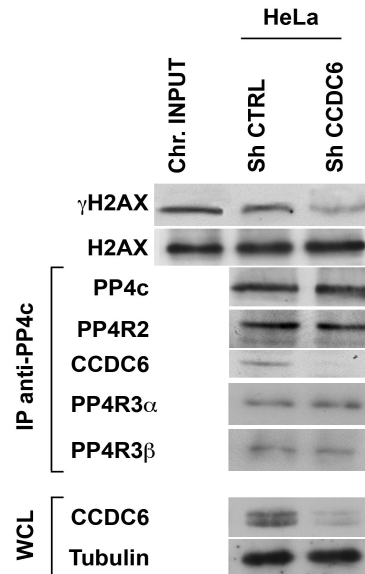


Fig.19 CCDC6 inhibits the phosphatase activity of PP4c.

PP4 complex immunopurified from HeLa cells transfected with CCDC6-specific shRNAs (shCCDC6) or with non-targeting control shRNAs (shCTRL), was incubated for 30 minutes at 30°C with γ H2AX-enriched chromatin purified from irradiated cells. The phosphatase reactions were followed by western blot and probed with the indicated antibodies.

γ H2AX intensity, from three independent experiments, was normalized against the intensity of non-phosphorylated H2AX, and against PP4c levels detected by immunoblot (Figure 20).

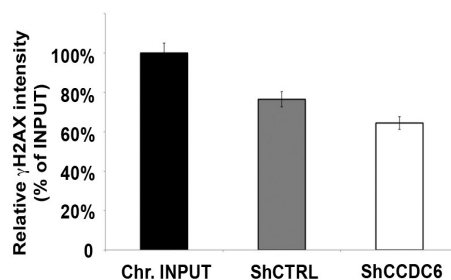


Fig.20 Histograms show the densitometric analysis of γ H2AX intensity, resolved on SDS-PAGE following phosphatase reactions, normalized against the intensity of non-phosphorylated histone H2AX, and against the PP4c levels on immunoblots. The histograms are representative of three independent experiments and error bars indicate the standard error mean.

In the next experiment, in order to perform a more accurate measurement of the phosphatase activity, we tested the activity of PP4 phosphatase on acid-extracted histones that we obtained from HeLa cells irradiated with a dose of 10 Gy to get quantified histone purification enriched in γ H2AX (Figure 21a and 21b).

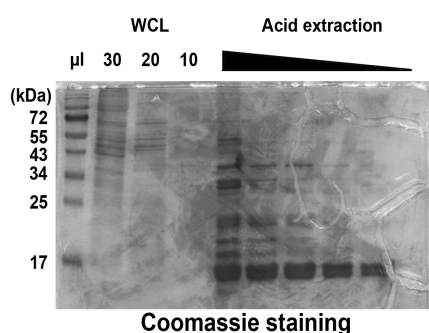


Fig.21a Irradiated HeLa cells (10Gy) were lysed, and histones were acid-extracted. Samples obtained from histone extraction (Acid extraction) and whole cell lysates were separated by SDS-PAGE and stained with Coomassie blue.

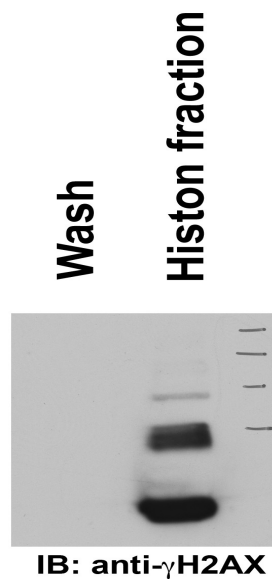


Fig.21b Mock (-) or irradiated HeLa cells (+, 10 Gy) were acid-extracted to purify total histones as in a). Various amount of proteins were separated by SDS-PAGE and transferred to nitrocellulose membranes that were hybridized with γ H2AX specific antibody.

In CCDC6-depleted HeLa cells (shCCDC6), proportional amount of the endogenous immunopurified PP4 complex showed increased activity on 3 μ g of acid-extracted histones compared to the activity that we observed in CCDC6-proficient HeLa cells (shCTRL), as revealed by the free phosphate detection with Malachite Green Phosphatase Assay (Figure 22).

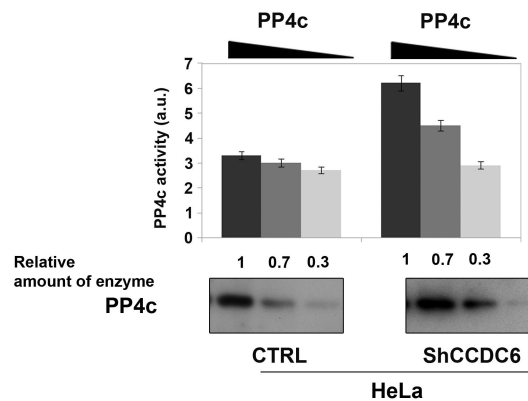


Fig.22

PP4c phosphatase was immunoprecipitated from shCCDC6 or shCTRL. 1, 0,7, 0,3 volumes of total PP4c immunoprecipitated from 3 mg of total cell extract were mixed with histones purified from cells exposed to 10 Gy IR and incubated in phosphatase buffer at 30°C for 30 minutes. Phosphatase reaction was terminated by the addition of 100µl of Malachite Green solution and absorbance was measured at 630 nm. After the phosphatase assay, the actual amount of PP4c in each immunoprecipitate was determined by Western Blotting with the indicated antibody. PP4c activity is represented in arbitrary units (a.u.) calculated as the ratio between released free phosphate (absorbance at 630 nm) and PP4c densitometric signal at western blot.

Lastly, we challenged proportional amount of immunoprecipitated PP4c with a synthetic phospho-peptide substrate (f.c. 175 µM) and we were able to determine a linear range of PP4c activity, by using the same assay (Figure 23).

To further understand the role of CCDC6 in PP4c activity modulation we utilized a human CCDC6- null cell line, the thyroid papillary carcinoma TPC-1 cells, that carry the RET/PTC1 oncogene and have lost by deletion the normal unrearranged CCDC6 allele (Jossart et al., 1996).

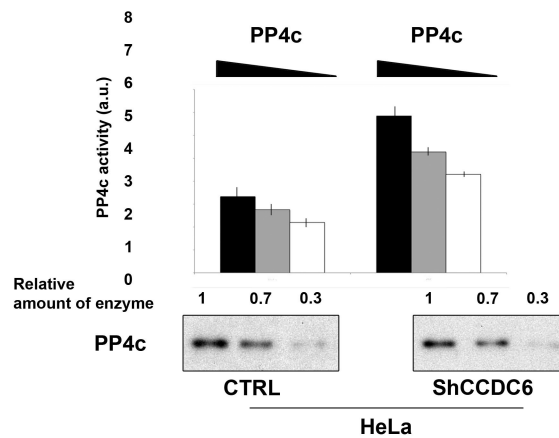


Fig.23

Enzymatic activity of PP4c immunopurified from HeLa cells transfected with CCDC6-specific shRNA (shCCDC6) or with non-targeting control sh-RNAs (shCTRL) was assessed by Malachite Green phosphatase assay. 1, 0,7 and 0,3 volumes of total PP4c immunoprecipitated from 3 mg of total cell extract were incubated with 175 μ M of RKpTIRR synthetic peptide for 30 minutes at 30°C. Phosphatase reaction was terminated by the addition of 100 μ l of Malachite Green solution and absorbance was measured at 630 nm. After the phosphatase assay, the actual amount of PP4c in each immunoprecipitate was determined by Western Blotting with the indicated antibody. PP4c activity is represented in arbitrary units (a.u.) calculated as the ratio between released free phosphate (absorbance at 630 nm) and PP4c densitometric signal at western blot.

Then, in TPC-1 cells, in which we transiently re-expressed the CCDC6 wild type, the phosphatase complex had poor activity on γ H2AX obtained by cells-fractionation (Figure 18), compared to the activity that immunopurified PP4c showed in TPC-1 cells overexpressing the CCDC6-truncated mutants (1-223; 1-101), both unable to interact with PP4c, as revealed by immunoblot (Figure 24).

The phosphatase reactions were followed by immunoblotting and probed with specific antibodies as indicated in figure 24. Immunopurified endogenous PP4R2, R3 α and R3 β were revealed at IB in TPC1 cells,

too.

γ H2AX intensity, from three independent experiments, was normalized against the intensity of non-phosphorylated H2AX, and against PP4c levels detected by immunoblot (Figure 25).

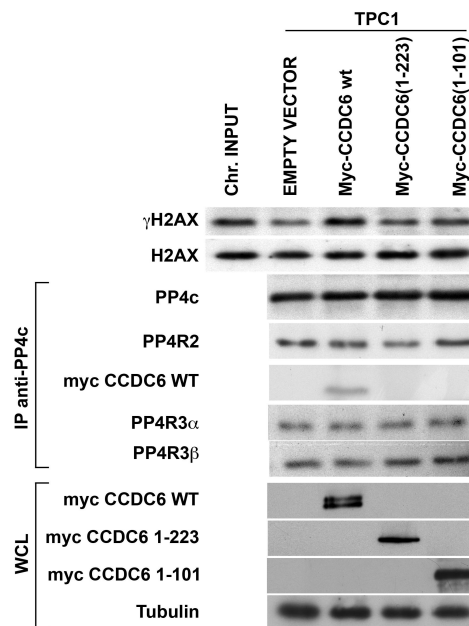


Fig.24 PP4 complex immunopurified from TPC-1 cells transfected with CCDC6 wt, CCDC6 (1-223) and (1-101) truncated mutants, was incubated for 30 minutes at 30°C with γ H2AX-enriched chromatin, purified from irradiated cells. The phosphatase reactions were followed by immunoblotting and probed with the indicated antibodies.

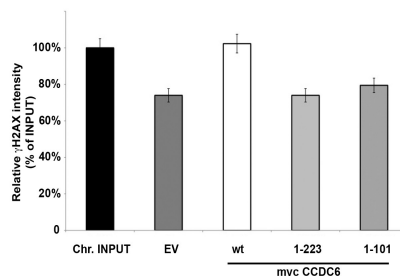


Fig.25 Histograms show the densitometric analysis of γ H2AX intensity, resolved on SDS-PAGE following phosphatase reactions, normalized against the intensity of non-

phosphorylated histone H2AX, and against the PP4c levels on immunoblots. The histograms are representative of three independent experiments and error bars indicate the standard error mean.

For an accurate measurement, in TPC-1 cells over-expressing CCDC6 wild type, proportional amount of the endogenous immunopurified PP4 phosphatase complex had poor activity on 3 μ g of acid-extracted histones compared to the activity that immunopurified PP4c showed in TPC-1 cells overexpressing the empty vector (Figure 26), as detected by Malachite Green Phosphatase assay.

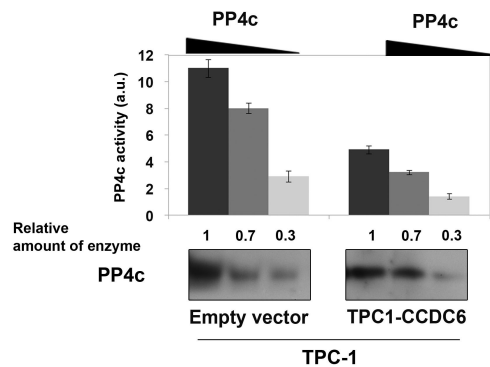


Fig.26 Enzymatic activity of PP4c immunopurified from TPC-1 cells transfected with epitope-tagged CCDC6 wt or empty vector, was determined as described in fig.22 and fig.23.

Finally, by using the same assay, we were able to determine, challenging proportional amount of immunoprecipitated PP4c with a synthetic phospho-peptide substrate (f.c. 175 μ M), a linear range of PP4c activity (Figure 27). Finally In figure 28 we show that by immunoprecipitation of PP4R2, as a means of immunopurifying PP4c in complex with regulatory subunits, we were able to modulate the phosphatase activity on 3 μ g of acid-extracted histones in Hela-CCDC6-depleted cells compared to Hela control cells.

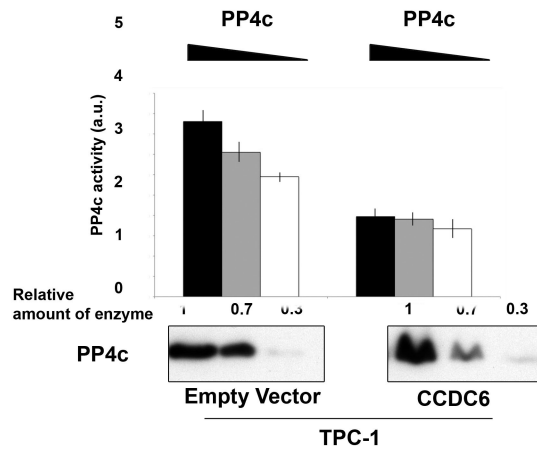


Fig.27 Enzymatic activity of PP4c immunopurified from TPC-1 cells transfected with epitope-tagged CCDC6 wt or empty vector, was determined as described in fig. 21-22.

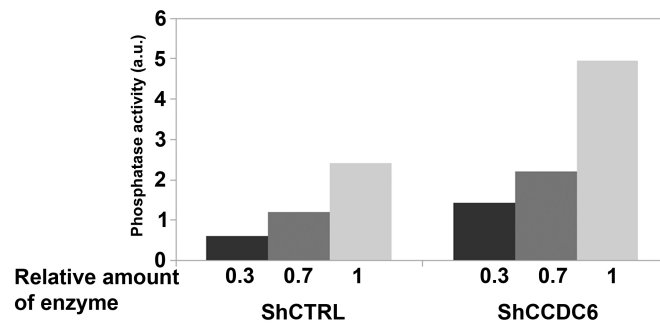


Fig.28 Phosphatase assay has been performed by immunopurifying PP4R2 as means of immunopurifying PP4c in complex with the regulatory subunits. The phosphatase complex by immunoprecipitating proportional amount of PP4R2, was immunoprecipitated from CCDC6 depleted and CCDC6 proficient HeLa cells and mixed with 3 μ g of acid extracted histones at 30°C for 30 minutes. Phosphatase reactions were terminated by the addition of 100 μ L of Malachite Green solution and absorbance was measured at 630nm.

3.3 Loss of CCDC6 affects H2AX phosphorylation after DSBs

We aimed to investigate the phosphorylation status on S139 of H2AX after genotoxic stress treatments in CCDC6-silenced clones, that we generated (Fig.29).

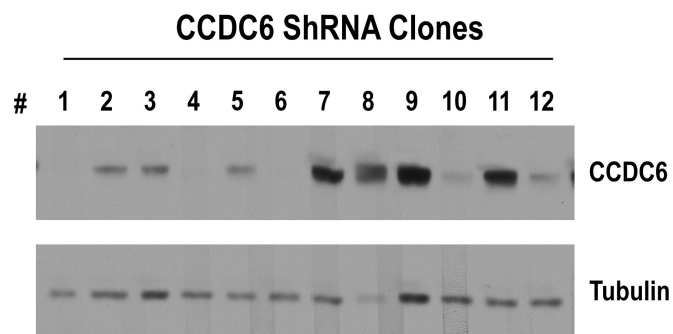


Fig.29 HeLa CCDC6 depleted clones obtained after transfection of a plasmid pool of mission ShRNA (pLKO.1 puro ShCCDC6 NM_005436, Sigma-Aldrich) after two weeks puromycin selection.

Thirty minutes after exposure to different doses of IR (1 and 5 Gy) we observed a barely detectable signal of γ H2AX in CCDC6-depleted HeLa clone#1, compared to clone#2, and to control HeLa cells (Figure 30). Thus, at the same dose of IR, the phosphorylation of H2AX appeared to correlate to the amount of CCDC6 (anti-CCDC6 blot at bottom of figure 30).

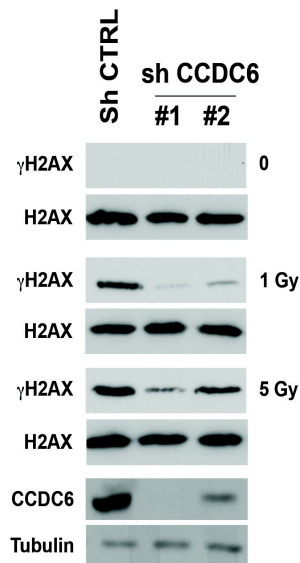


Fig.30 Loss of CCDC6 affects H2AX phosphorylation after genotoxic stress

In the WCL of two representative CCDC6-depleted HeLa clones (shCCDC6 #1 and #2) and control HeLa cells (shCTRL), thirty minutes after 1-5 Gy IR exposure, the phosphorylation of H2AX was detected with the mouse anti- γ H2AX by western blot. Anti-total H2AX was used as a loading control. The immunoblots with anti-CCDC6 and anti-tubulin antibodies were shown in the bottom.

By immunofluorescence, CCDC6-depleted HeLa clone#1 cells showed few γ H2AX positive foci after thirty minutes exposure to different doses of IR (1 and 5 Gy), compared to control HeLa cells (Figure 31).

The quantization of γ H2AX positive foci is shown in the histograms of Figure 32.

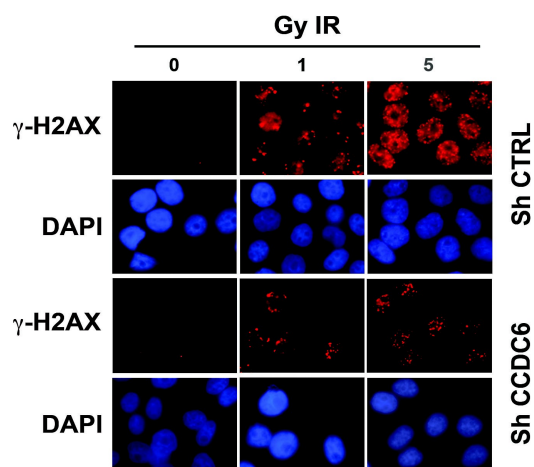


Fig.31 Immunofluorescence analysis of γ H2AX foci in CCDC6-depleted clone #1 (shCCDC6) and control HeLa cells (shCTRL), thirty minutes after 0.5, 1, and 5 Gy IR exposure. Nuclei were counterstained with DAPI. Magnification was at 63x.

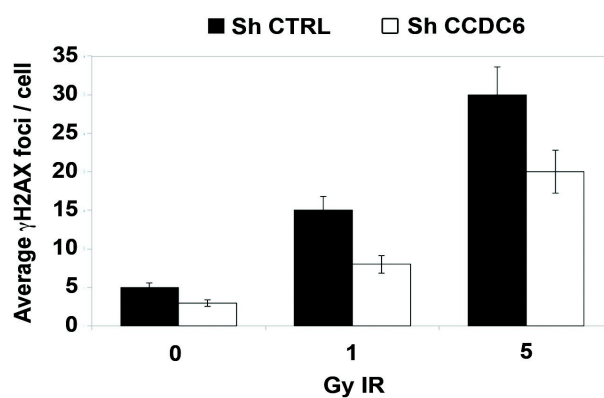


Fig.32 Quantification of γ H2AX foci number.

At least 300 cells were analysed per experiment. Error bars indicate the standard mean error.

Interestingly, at single time point, in CCDC6-depleted cells, the re-expression of CCDC6wt, but not of CCDC6T434A, mutated in the ATM phosphorylation site, restored γ H2AX levels at WB after treatment with 1 μ M and 2,5 μ M of Etoposide (Figure 33) in a dose dependent manner.

The saturation of γ H2AX levels at 5 μ M suggests that CCDC6 is able to modulate γ H2AX levels in presence of low DNA damage.

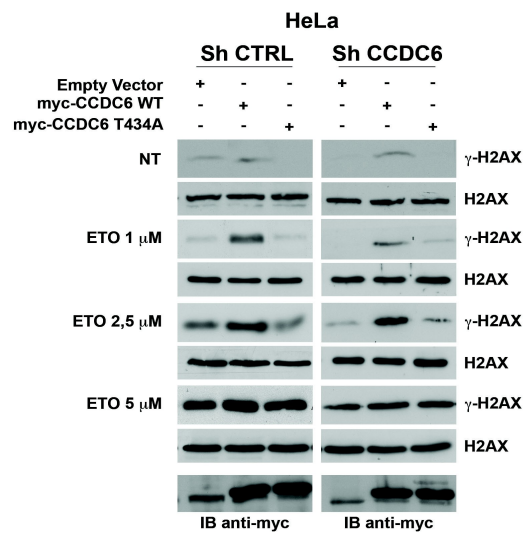


Fig.33 CCDC6-depleted clone #1 (shCCDC6) and control HeLa cells (shCTRL) transfected with expression vectors encoding CCDC6wt, CCDC6T434A or the empty vector were treated with etoposide at 1, 2,5 and 5 μ M for 8 h and western blot analysis of γ H2AX and myc-tagged proteins were performed.

At several time point over time after exposure to a fixed dose of IR (1Gy), we observed that CCDC6 knock-down in HeLa cells affected the H2AX phosphorylation compared to HeLa control cells, in presence of phosphorylated ATM at p-Ser-1981 that correlate with normal ATM activation (Lee&Paull, 2005; Daniel, 2007; Reinhardt and Yaffe, 2009) (Figure 34).

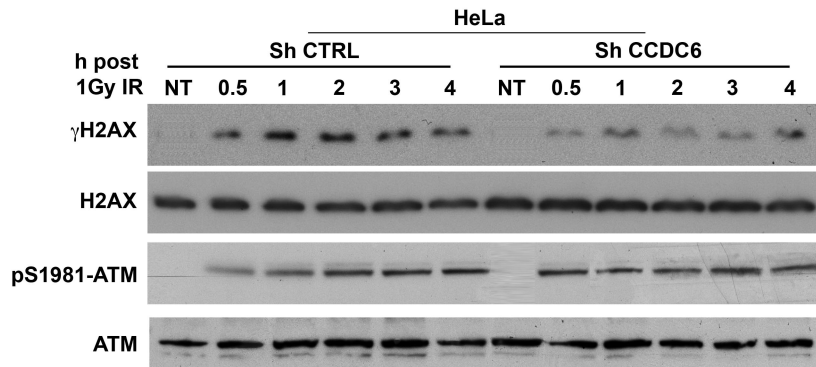


Fig.34 PP4c depletion rescues γ H2AX levels in CCDC6 silenced cells

H2AX phosphorylation detection with mouse anti- γ H2AX by WCL analysis of CCDC6-depleted HeLa clone #1 (shCCDC6) and control cells (shCTRL) at several time point as indicated after exposure to 1Gy of IR. Anti total H2AX is shown as loading control. The anti-pSer1981-ATM and the ATM hybridization are shown at bottom of the figure.

Next, we examined the impact of PP4c on the levels of γ H2AX that we observed in shCCDC6, compared to control cells, upon IR exposure. By using sh-RNA-mediated depletion of PP4c in CCDC6-proficient or CCDC6-depleted HeLa cells we checked the levels of γ H2AX after 1Gy IR exposure. As shown in figure 35 depletion of PP4c rescued total levels of γ H2AX in CCDC6-depleted cells, upon IR.

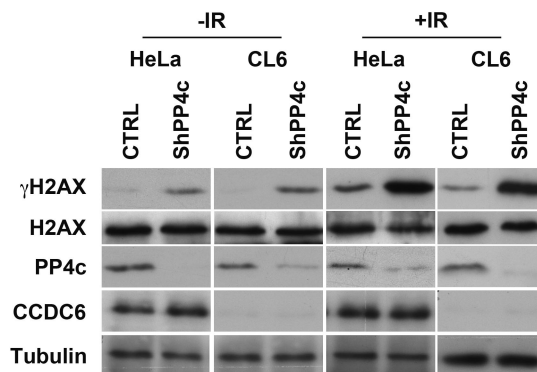


Fig.35 shCCDC6 and shCTRL HeLa cells were depleted of PP4c by shRNA (48 hours) and were exposed to 1 Gy of IR, as indicated (-/+). Phosphorylation of H2AX, PP4c, CCDC6, total H2AX and tubulin amount were revealed at IB of WCL.

Moreover, in order to show that CCDC6 impacts PP4c activity in the context of the DDR, we investigated the phosphorylation status of another PP4c substrate, the DNA repair protein RPA2: in CCDC6-depleted HeLa cells after treatment with 1 μ M of Etoposide at several time point following double thymidine block, the pRPA2 protein levels were not affected by CCDC6 depletion, whereas the levels of γ H2AX were barely detectable in shCCDC6 cells, compared to controls (Figure 36), suggesting a functional activity upon CCDC6 – PP4c interaction towards one particular substrate the histone γ -H2AX.

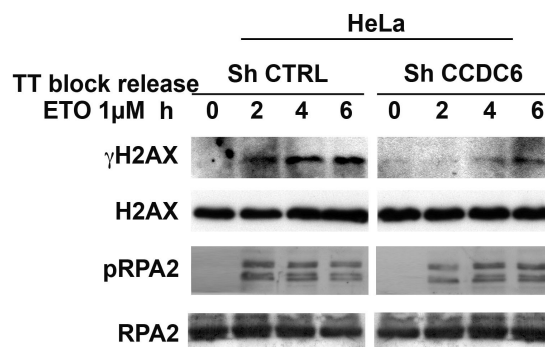


Fig.36 In the cell extract of CCDC6-depleted clone #1 (shCCDC6) and control HeLa cells (shCTRL), after double thymidine block (TT block) and release in presence of 1 μ M Etoposide at several time point, as indicated, phosphorylation levels of H2AX and of RPA2 were revealed with anti- γ H2AX and with anti-p-RPA2 by western blot. Anti-total H2AX and anti-total RPA were shown as loading control.

It has been reported that RPA2 interacts with PP4c exclusively upon Camptothecin (CPT) treatment. In order to evaluate if the loss of CCDC6 could impact the level of pRPA2 upon replicative stress, in CPT-treated CCDC6 depleted cells, we evaluated the levels of pRPA2 that

were high and have comparable levels with the control cells; interestingly, upon CPT treatments the γ H2AX levels were rather undetectable in CCDC6-deficient cells, compared to CCDC6 proficient cells, suggesting that CCDC6 is able to negative modulate the PP4c activity upon replicative stress, too (Figure 37).

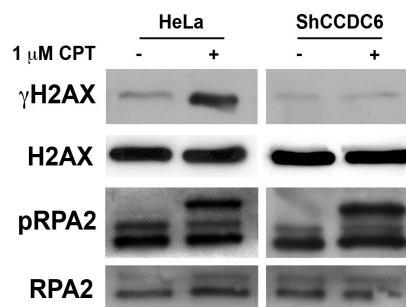


Fig.37 In the cell extract of CCDC6-depleted clone #1 (shCCDC6) and control HeLa cells (shCTRL), in presence of 1 of Camptothecin (CPT) phosphorylation of H2AX and of RPA2 were revealed with the mouse anti- γ H2AX and with anti-p-RPA2 by western blot. Anti-total H2AX and anti-total RPA were shown as loading control.

3.4 Loss of CCDC6 affects the DNA damage induced G2-arrest

In order to investigate if the CCDC6 loss could affect the cell cycle progression in presence of DNA damage, HeLa CCDC6-depleted cells (shCCDC6) were synchronised by double thymidine block and then released in 1 μ M etoposide. In these cells, compared to controls (shCTRL) we observed failure to arrest in G2 and ability to progress into cell cycle, as measured by FACS analysis at different time point (Figure 38).

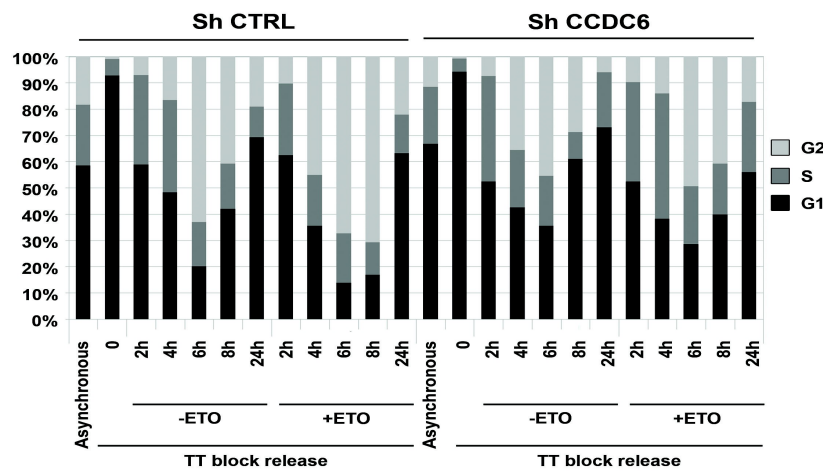


Fig.38 Loss of CCDC6 affects the DNA damage induced G2 arrest.

Cell cycle distribution of the stable HeLa CCDC6 silenced clone #1 (shCCDC6) and control HeLa cells (shCTRL) after release from double thymidine block (TT-block) in the presence of 1 μ M Etoposide.

Moreover, in order to investigate if CCDC6 could be involved in the recovery from the DNA damage induced G2-checkpoint, control and CCDC6-depleted HeLa cells were synchronised with double thymidine block, treated for 1 hour with 1 μ M etoposide and released in 50 ng/ml of Nocodazole. Sampling of cells taken at several time showed that control cells entered mitosis at 6-8 hours from release, whereas after etoposide treatment the mitotic entrance resulted strongly delayed. CCDC6-depleted etoposide-treated cells started to enter mitosis at 4-6 hours after the initial arrest, earlier than control cells, as revealed by WB levels utilizing the anti-phospho-S/T-MPM2 antibody, able to recognize specifically the mitotic phosphosubstrates (Figure 39) (Tsai *et al*, 2005).

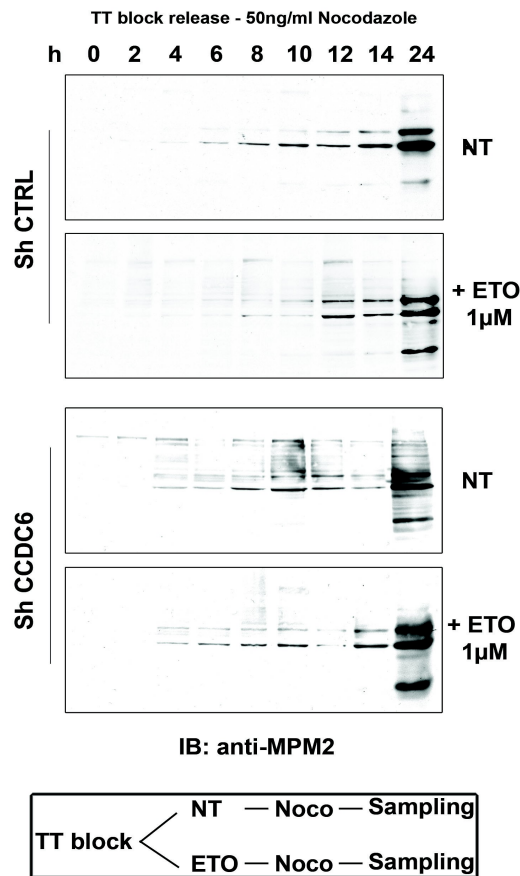


Fig.39 Mitotic entry after TT-block and release in 1µM Etoposide for one hour where indicated, in presence of 50 ng/ml Nocodazole was monitored by western blot using the anti-p-S/TMPM2 antibody. Sketch of the cells treatment is shown in the bottom panel.

Percent of mitotic cells was also evaluated by FACS analysis of the anti-pSer10- histone H3 antibody positive staining (Figure 40), and by scoring for mitotic features (Figure 41).

These results suggest that the depletion of CCDC6 by shRNA may induce DNA-damage tolerance and a deficient DNA damage checkpoint. To exclude an off-target effect, we repeated these experiments using

either additional shCCDC6 clones (Figure 29) or previously validated siRNA (Merolla *et al.*, 2007) and we obtained similar results (data not shown).

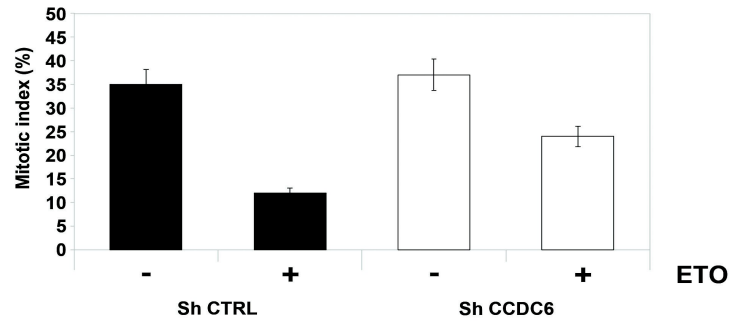


Fig.40 Percentage of mitotic cells was monitored, by FACS analysis, with anti-p-Ser10-histone H3 staining, in stable CCDC6 silenced and control HeLa cells treated as in (37) at 8 hours, as indicated.

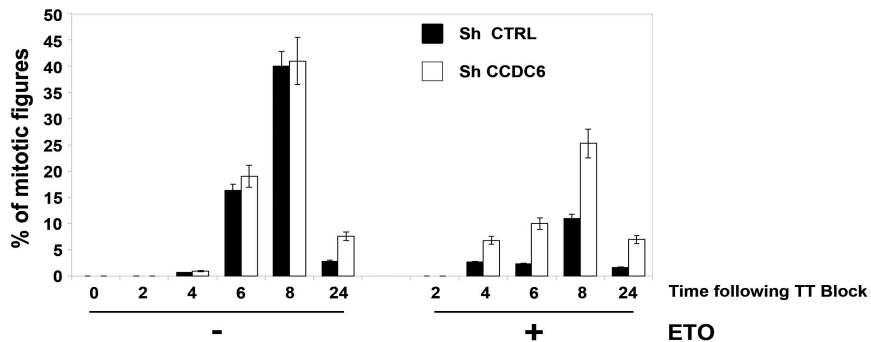


Fig.41 in HeLa CCDC6 silenced clone #1 (shCCDC6) and control HeLa cells (shCTRL) growth on coverslips and collected at several time points following G1/S synchronization by double thymidine block (TTblock) in the presence of 1 μ M Etoposide, as indicated, mitotic figures were counted after nuclear counterstaining with Dapi. Magnification was at 40x. The histograms are representative of three independent experiments and error bars indicate the standard error mean.

3.5 CCDC6 loss affects DNA repair

A cross talk between checkpoints and DNA repair mechanisms has been reported (Lazzaro *et al.*, 2009). In order to understand if the DSBs induced from exogenous sources, such as IR or chemical agents, could be unrepaired or misrepaired in absence of CCDC6 we applied pulsed-field gel electrophoresis (PFGE) that allows separation of greater DNA sizes excised from genomic DNA by DSBs, and then represent a good system for studying DNA repair, by observing the reduction in migrating DNA when cells are allowed a period of repair following genotoxic insult (Speit and Hartmann, 1995; DiBiase *et al.*, 1999). Therefore, we wanted to check the recovery time of DSBs in CCDC6-knock down HeLa cells, compared to controls, upon exposure to 10 Gy IR and collection at various time point for embedding in low melting agarose plugs. DSBs from damaged cells, together with un-damaged DNA, is shown and we can appreciate that CCDC6 depleted cells get the ability to repair the damaged DNA in a shorter time compared to control (Figure 42).

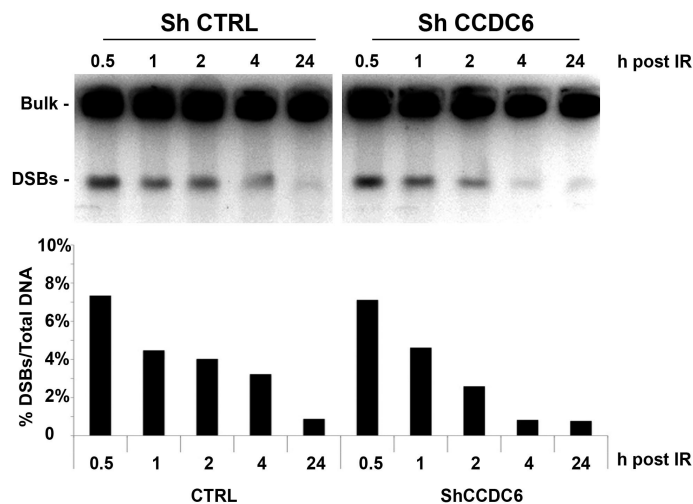


Fig.42 Loss of CCDC6 affects DSBs repair.

Detection of DSBs by PFGE. After 10 Gy IR exposure CCDC6-depleted (shCCDC6) and CCDC6-proficient (shCTRL) HeLa cells have been collected at different time

points (1, 2, 4, 24 hours). Densitometric analysis of DSBs bands were plotted as percentage of total DNA.

Finally, in order to evaluate the impact of CCDC6 on the radiation response we performed clonogenic survival assay on the CCDC6-depleted cells and control cells after exposure to a range doses of IR (0, 2, 4, 6, 8 Gy) and we observed that the silenced clones were more resistant to the genotoxic stress than the control cells at 14 days (Figure 43).

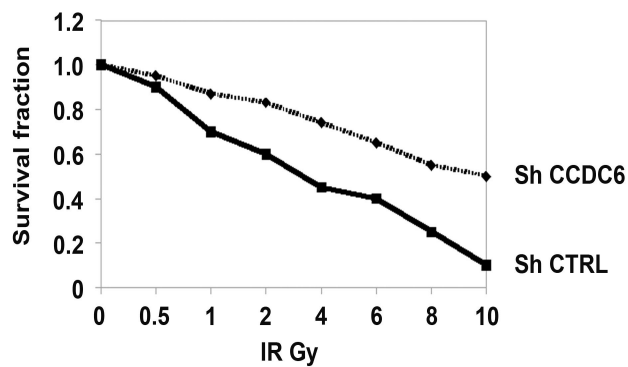


Fig.43 Clonogenic assays of stable CCDC6 silenced and control HeLa cells were assayed by crystal violet staining, after 14 days following exposure to IR at the indicated range doses (0, 2, 4, 6, 8 Gy). The curves show the survival fractions normalized against non-irradiated cells.

4. DISCUSSION

In the present study we have investigated the physiological role of CCDC6 in DNA-damage response and repair through its interaction with PP4c.

We confirmed the predicted interaction between CCDC6 and the catalytic subunit of Protein Phosphatase 4 (Ewing *et al.*, 2007; Chen *et al.*, 2008) and we observed that CCDC6 negatively modulates the phosphatase activity of PP4c on γ H2AX, one of the earliest markers of DNA doublestrand breaks.

We found that CCDC6 interacted with PP4c but not with PP2A, as also reported (Glatter *et al.*, 2009). Both PP2A and PP4 belong to the PP2A-like phosphatase family and are reported to dephosphorylate γ H2AX. However, it is believed that each phosphatase plays a different physiological role, with PP2A functioning mainly after DNA damage, (Chowdhury *et al.*, 2005; Paull 2006; Keogh *et al.*, 2006), and PP4c mostly involved in replication induced DNA damage and in DNA damage checkpoint recovery (Chowdhury *et al.*, 2008; Nakada *et al.*, 2008). Recently, PP6c and Wip1 have also been found to exert an important role in the removal of γ H2AX from chromatin, (Douglas *et al.*, 2010; Macurek *et al.*, 2010) whereas PP1c has been reported to be not able to affect γ H2AX levels (Nakada *et al.*, 2008). Thus, several phosphatases (PP2a, PP4c, PP6c, Wip1) participate directly or indirectly in the dephosphorylation of γ H2AX. It is still not clear what the exact contribution of each phosphatase is, but the emerging data suggest some level of redundancy as well some context-dependent specificity (Freeman & Monteiro, 2010).

The removal of γ H2AX from sites of DNA damage is tightly regulated; it closely correlates with DNA repair and most likely relies on phosphatases activity. Indeed, PP4c functions in the termination of the

DNA damage checkpoint signalling (Nakada *et al.*, 2008).

In this study we observed that, upon exposure to genotoxic stress, the CCDC6 loss or inactivation, as reported in some human cancer, increases dephosphorylation of γ H2AX in a PP4c-dependent manner, resulting in a deficient DNA-damage checkpoint recovery and a premature release from G2 arrest imposed by DNA damage. These data correlate with results recently reported about overexpression of Wip1, a direct phosphatase of γ H2AX, that leading to low levels of γ H2AX in response to DNA damage prevents checkpoint activation and leads to checkpoint override. Indeed, cells expressing Wip1 and showing low levels of γ H2AX fail to activate the checkpoint and progress to mitosis (Makurek *et al.*, 2010). Interestingly, the depletion of PP4c in CCDC6 silenced cells rescued the levels of γ H2AX, suggesting a functional link between CCDC6-PP4c and γ H2AX on sensing the DNA damage.

Moreover, we found that in presence of DNA-damage loss of CCDC6, keeping low levels of γ H2AX affects the repair of DSBs, as revealed by PFGE experiments. We hypothesize that in cells with low CCDC6 as the DNA-damage checkpoint weakens, a faster and less accurate repair pathway, such as NHEJ, might operate in these conditions, potentially explaining the different recovering time, observed with the PFGE between CCDC6 proficient and CCDC6 depleted cells. This observation need further investigations.

Our data indicate that in cells where CCDC6 is loss, the increased activity of PP4c, as we detected by phosphatases assays, results in low levels of γ H2AX, but it could be also possible that these effects might be dependent from inactivation of kinases responsible for γ H2AX phosphorylation. To address this point we checked the pSer-1981 ATM which resulted active upon IR exposure in CCDC6 depleted and CCDC6 proficient HeLa cells.

PP4 is an obligate heterodimer and heterotrimer (Chen *et al.* 2008) with

at least six regulatory subunits that are believed to confer substrate specificity (Chowdhury *et al.* 2008, Nakada *et al.* 2008). We found that CCDC6 is important for the activity of the PP4-R2-R3 complex on the dephosphorylation of H2AX, but it was not affecting the phosphorylation status of the DNA repair protein RPA2, another PP4c substrate, upon genotoxic or replicative stress. These experiments suggested that the functional activity upon CCDC6-PP4c interaction is directed towards one particular substrate, the histone γ H2AX, not only after genotoxic stress exposure, but also upon replicative stress. Nevertheless, it will be interesting to investigate if CCDC6 could influence the activity of the specific PP4 complex on other known phospho-substrates, such as HDAC3, or JNK, under different stress conditions (Zhang *et al.*, 2005; Zhou G *et al.*, 2002).

In the present study we hypothesize that CCDC6 is able to modulate PP4c at the sites of DNA damage, as the CCDC6 chromatin binding increased after genotoxic stress exposure (Figure 18b) and, also the CCDC6 colocalization with an established marker of DNA damage, such as MDC1, was seen in some foci (data not shown). As CCDC6 primary structure lacks a canonical DNA-binding motif these observations might uncover an unexpected function of the protein at chromatin level. In addition, as CCDC6 binds several interactors through a large coiled-coil domain, several post-translational modified residues and a proline-rich region, we can configure it as a scaffold protein.

On the basis of the data we collected in this study we may also envisage a mechanism that could explain the apoptotic phenotype that we previously reported in CCDC6 overexpressing cells: CCDC6 by negatively regulating the PP4c phosphatase activity maintains high levels of γ H2AX, with hyperactivation of the G2/M checkpoint and an increase in the apoptotic rate (Celetti *et al.* 2004, Fernandez-Capetillo *et al.* 2004). Moreover, in TPC-1 cells that carry the RET/PTC1 oncogene

and have lost the CCDC6 unrearranged allele, we observed a decreased PP4c phosphatase activity upon re-expression of wild-type CCDC6.

The overexpression of protein phosphatase PP4 has already been reported in some primary tumours (Wang *et al.* 2008) and it would be interesting to investigate the correlation between the loss or inactivation of CCDC6, as reported in some tumors by the Cancer Genome Atlas (<http://tcga.cancer.gov>) and the increase of PP4c phosphatase activity with the alteration of the G2 checkpoint maintenance and recovery in human cancer.

CCDC6 gene is often found rearranged to RET and to genes other than RET in thyroid and nonthyroid human neoplastic diseases (Kulkarni *et al.* 2000, Schwaller *et al.* 2001, Puxeddu *et al.* 2005, Drechsler *et al.* 2007). Since in all these tumours the fusion results in the loss of function of one allele, and in some cases also of the normal unrearranged allele, it is reasonable to hypothesize that this loss might disrupt the growth balance contributing to neoplastic transformation.

5. CONCLUSIONS

In conclusion the data we obtained about CCDC6 as stress response protein that preserve genome stability upon interaction with PP4c, make CCDC6 an attractive candidate to help premature tumour cells overcome a DDR-dependent barrier against tumor progression (Halozonetis, 2008).

The loss of checkpoint function and of repair accuracy, which we observed in absence of CCDC6, might favour genome instability and might represent an early independent event of a multistep carcinogenetic process in primary tumours.

6. MATERIALS AND METHODS

6.1 Materials, antibodies

Etoposide [4'-Demethylepipodophyllotoxin 9-(4,6-O-ethylidene- β -Dglucopyranoside), VP-16-213] is an antitumor agent that complexes with topoisomerase II and DNA to enhance double-strand and single-strand cleavage of DNA and reversibly inhibit religation.

Camptothecin (CPT) is a cytotoxic quinoline alkaloid which inhibits the DNA enzyme topoisomerase I (topo I). CPT binds to the topo I and DNA complex (the covalent complex) resulting in a ternary complex, and thereby stabilizing it. This prevents DNA re-ligation and therefore causes DNA damage which results in apoptosis.

Hydroxyurea is an antineoplastic drug. Inactivates ribonucleoside reductase by forming a free radical nitroxide that binds a tyrosyl free radical in the active site of the enzyme. This blocks the synthesis of deoxynucleotides, which inhibits DNA synthesis and induces synchronization or cell death in S-phase.

Crystal violet also known as *Methyl Violet 10B*, *hexamethyl pararosaniline chloride*, or *pyocyanin(e)* is a triarylmethane dye. as a means of avoiding UV-induced DNA destruction when performing DNA cloning in vitro.

Etoposide, camptothecin, hydroxyurea, crystal violet, thymidine and puromycin were obtained from Sigma Chemical Co. (St Louis, MO, USA); Blasticidin was from Invitrogen (Carlsbad, CA, USA), Deoxycytidine hydrochloride from Fluka. Okadaic acid was from Biomol International (Farmingdale, New York).

We employed the following antibodies: mouse anti- γ H2AX (Upstate, clone JBW301), rabbit anti-H2AX (Cell Signaling), rabbit anti-PP4C

(Bethyl, A300-835A), rabbit anti-PP4R2 (Bethyl, A300-838A), rabbit anti-PP4R1 (Bethyl, A300-836A), rabbit anti-PP4R3a (Bethyl, A300-840A), rabbit anti-PP4R3b (Bethyl, A300-842A), rabbit anti-PP4R4 (abcam, ab111419), rabbit anti-PPM1D (Bethyl, A300-664A), rabbit anti Phospho RPA32 (S33) (Bethyl, A300-264A), rabbit anti RPA32 (Bethyl, A300-244A), rabbit anti-PPP6C (Bethyl, A300-844A), mouse anti-CCDC6 (abcam ab56353), mouse anti-phospho-Ser/Thr-Pro, MPM2 (Upstate, 05-368), mouse anti-phosphohistone H3 (Ser 10, Cell Signaling, clone 6G3), rabbit anti-MDC1, (abcam, ab 11171), mouse anti-phospho-ATM (Ser1981) (Cell Signaling, #4526) antibodies.

6.2 Cell culture, plasmids and transfection

TPC-1 and 293T cells were maintained in Dulbecco.'s modified Eagle.'s medium supplemented with 10% fetal bovine serum; HeLa cells were maintained in RPMI (Gibco, Paisley, UK), supplemented with 10% fetal bovine serum.

GST-CCDC6 fusion proteins production, small inhibitor duplex RNAs targeting human CCDC6, pCDNA4ToA-CCDC6wt, 1-223, 1-101 have been described elsewhere (Merolla et al., 2007).

The Fugene reagent (Roche) was used to transfect cells accordingly to the manufacturer's instructions.

6.3 RNA interference and short hairpin mission

Mission shRNA (pLKO.1 puro) were from Sigma-Aldrich, Inc. In order to obtain CCDC6 stably depleted Hela cells were transfected with the plasmid pool (shCCDC6, NM_005436) or a pool of non-targeting vectors (sh control) by the Nucleofector transfection system. For PP4c, PP4R2 transient silencing the plasmid pool of PP4c mission shRNA bacterial glycerol stock (NM_002720) and the sh PP4R2 (NM_174907) were transfected. Silencing of PP4R2 and PP4C were purchased from

MISSION shRNA Plasmid DNA from Sigma-Aldrich and were transfected using Fugene-HD (Roche). All siRNAs employed in this study were purchased from Sigma Aldrich. All RNAi transfections were performed using Oligofectamine Reagent (Invitrogen).

Individual siRNA are PPAR1: 5'-GGAGCUCAUUGAACGAUUUUU-3' and 5'-AAAAUCGUUCA AUGAGCUCC-3'.

PP4R4: #N1 5'- GAACAAGUGUGAUUGCAAUU-3' and 5'- AAUUUGCAAUCACACUUGUUC-3';

#N2 5'- UGAAAGGGCUGUUUAUCUGUU-3' and 5'- AACAGAUAAACAGCCCUUUCA-3';

#N3 5'- GAUUGACAGUCGAUGAAGAAUCG-3' and 5'- AAUCUUCAUCGACUGUCAAUCCG-3';

#N4 5'- GCGAUGGAUUUCAGUCAGAUU-3' and 5'- AAUCUGACUGAAAUCCAUCGC-3'.

PP4R3 α : 5'- UGAAUUAAGUCGCCUUGAAUU-3' and 5'- UUCAAGGCGACUUA AUUCAUU-3'.

PP4R3 β : 5'-CCAUCUAUAUUGCGUAGUAUU-3' and 5'- UACUACGCAAUAUAGAUGGUU-3'.

PP4R2#N1

CCGGGCCCTGTAAGTAGTAGTTCTTCTCGAGAAGA ACTACTACTTAC
AGGGCTTTTT

PP4R2 #N2

CCGGCGTGAAACAGAAGAATTAGTACTCGAGTACTAATTCTTCTGTT
TCAGGTTTTT.

All experiments were performed from 48 to 72 h post transfection.

6.4 Western Blotting

Western Blotting and immunoprecipitates was performed as described (Laemli, UK, 1970; Towbin H, Staehelin, and Gordon J, 1979). Blots were hybridized with antibodies to the indicated proteins and then with

their corresponding species-specific horseradish peroxidase-conjugated secondary IgG and visualised using the ECL chemi-luminescence system (Amersham/Pharmacia)

6.5 Flow cytometry

Cells at 70% confluence were harvested, fixed in ethanol for 1 h at -20°C, rehydrated in PBS for 1 h at 4°C, and then treated with RNase A (100 U/ml) for 30 min. Propidium iodide (25 mg/ml) was added to the cells for 30 min in the dark at room temperature. The percentage of the M-phase cells was determined by staining with PI and antibody to phospho-histone H3 (P-H3) (Cell Signaling, Beverly, MA, USA), followed by FITC-conjugated secondary antibody (Jackson ImmunoResearch Laboratories, West Grove, PA, USA). Samples were analysed with a FACScan flow cytometer (Becton Dickinson, San Jose, CA, USA) using an argon-ion laser tuned to 488nm measuring forward and orthogonal light scatter, and red fluorescence measuring area and either peak of the fluorescent signal. Data were analysed with Modfits software.

6.6 Indirect Immunofluorescence

The indirect immunofluorescence was performed as follow. For immunofluorescence staining the CCDC6 gene product was detected with rabbit polyclonal antibody anti-CCDC6 at 1:50 dilution applied 1h at 37 °C in a humidified chamber and a fluorescein isothiocyanate (FITC)-conjugated donkey anti-rabbit secondary IgG antibody at 1:50 dilution (Jackson ImmunoResearch Laboratories Inc., West Grove, OK, USA). For immunofluorescence staining, exogenous myc-H4wt and myc-H4T434A were detected with mouse monoclonal antibody anti-myc (Santa Cruz) at 1:50 dilution applied 1h at 37 °C in a humidified chamber and a fluorescein isothiocyanate (FITC)-conjugated donkey anti-mouse secondary IgG antibody at 1:50 dilution (Jackson

ImmunoResearch Laboratories Inc., West Grove, OK, USA). After washing three times with PBS, the slides were washed with Hoechst 33258 (final concentration, 1 µg/mL; Sigma-Aldrich) to stain nuclei and then mounted in aqueous medium (Sigma, Milan, Italy).

6.7 Chromatin extraction

2×10^6 cells were lysed in 100 µl of CSK buffer (10 mM Pipes-KOH pH 6.8, 100mM NaCl, 300mM Sucrose, 1.5 mM MgCl₂) containing 0.5% TritonX100, supplemented with Proteinase and Phosphatase inhibitors. Lysates were incubated on ice for 10 minutes and then centrifuged at 1500 x g for 5 minutes at 4°C. Supernatant was removed, pellets were washed with 1 ml of lysis buffer and centrifuged again. Pellets were incubated in 100 µl of CSK buffer containing 1U/µl of Benzonase (Novagen) for 1h at room temperature. After centrifugation supernatant was collected, boiled in 1X Laemli loading dye.

6.8 Phosphatase Assays

Chromatin fractions were purified by HeLa cells after 10 Gy IR exposure as indicated above. Crude histones were isolated by acidic extraction from cells exposed to IR (10Gy, 1h) using a Histone purification kit (Active Motif, Carlsbad, CA, USA). 293T cells were lysed in buffer containing 60 mM Tris-HCl (pH 8.0), 1% Nonidet P-40, 120 mM NaCl, 1mM EDTA, 6 mM EGTA, 1 mM dithiothreitol, 50 µM p-amidinophenylmethanesulfonyl-Fluoride and 2 µg/ml aprotinin. Endogenous PP4 was immunoprecipitated with an anti-PP4C antibody. The immunoprecipitates were washed three times in washing buffer. Phosphatase assays were performed incubating the PP4C immunoprecipitated with purified chromatin fraction or mixed with 3 micrograms of acid-extracted histones in 40 µl of assay buffer (50 mM Tris pH 7.0, 0.1 mM CaCl₂, and 1 mM MnCl₂) at 30 °C for 30 min

(unless otherwise indicated). Buffer plus chromatin fraction was used as a negative control, boiled in a SDS-PAGE loading buffer for 5 min, resolved by 15% SDS-PAGE, transferred to nitrocellulose membranes, and then subjected to Western blotting with the indicated antibodies. Enzymatic activity of PP4c on acid-extracted histones or on synthetic RKpTIRR phosphorylated substrate was detected by the Malachite Green phosphatase assay, according to Manufacturer's protocol (Upstate Biotechnology Inc, Lake Placid, NY).

6.9 G2/M checkpoint recovery assay.

The cells were synchronized in G1/S phase by double thymidine-block. Nocodazole was used at 50 ng/ml for 16 hours, before cells releasing. For FACS analysis of phospho-S/T-MPM2 staining, cells were fixed with 3% paraformaldehyde at various time points, permeabilized with 70% methanol and blocked with FACS incubation buffer (0.5% BSA in PBS) for 10 min.

6.10 DSBs detection by PFGE

Standard conditions for the DSBs compaction in one band have been adapted to the CHEF DRIII apparatus (BIORAD) from Hanada *et al.*, 2007.

6.11 Clonogenic assays

Cell lines exposed to a range of doses of ionizing irradiation (0–8 Gy) were plated in triplicate at limiting dilutions into six-well plates, incubated for 24 h, and then followed by incubation for 2 weeks. Before counting colonies, cells were fixed in 95% methanol and stained with crystal violet.

A population of more than 50 cells was counted as one survived colony. The mean colony counts standard errors are reported.

7. REFERENCES

Bakkenist CJ, Kastan MB, (2003). DNA damage activates ATM through intermolecular autophosphorylation and dimer dissociation. *Nature* 421(6922):499-506.

Bane A, Brown L, Carter J, Cote C, Crider K, de la Forest S, Livingston M, Montero D. (2003). Life and death decisions: America's changing attitudes towards genetic engineering, genetic testing and abortion, 1972-98. *Int Soc Work. Apr*;46(2):209-19.

Bartek J, Lukas J. (2007). DNA damage checkpoints: from initiation to recovery or adaptation. *Curr Opin Cell Biol.* 19(2):238-45.

Beausoleil SA, Jedrychowski M, Schwartz D, Elias JE, Villén J, Li J, et al. (2004). Large-scale characterization of HeLa cell nuclear phosphoproteins. *Proc Natl Acad Sci U S A* 101(33):12130-5.

Brewis ND, Street AJ, Prescott AR, Cohen PT, (1993). PPX, a novel protein serine/threonine phosphatase localized to centrosomes. *EMBO J. Mar*;12(3):987-96.

Brill LM, Salomon AR, Ficarro SB, Mukherji M, Stettler-Gill M, Peters EC. (2004). Robust phosphoproteomic profiling of tyrosine phosphorylation sites from human T cells using immobilized metal affinity chromatography and tandem mass spectrometry *Anal Chem* 76(10):2763-72.

Burma S, Chen BP, Murphy M, Kurimasa A, Chen DJ, (2001). ATM phosphorylates histone H2AX in response to DNA double-strand breaks. *J Biol Chem.* Nov 9;276(45):42462-7. Epub 2001 Sep 24.

Caudill CM, Zhu Z, Ciampi R, Stringer JR, Nikiforov YE, (2005). Dose-dependent generation of RET/PTC in human thyroid cells after in vitro exposure to gamma-radiation: a model of carcinogenic chromosomal rearrangement induced by ionizing radiation. *J Clin Endocrinol Metab* 90, 2364-2369.

Celetti A, Cerrato A, Merolla F, Vitagliano D, Vecchio G, Grieco M. (2004). H4(D10S170), a gene frequently rearranged with RET in papillary thyroid carcinomas: functional characterization. *Oncogene* 23(1):109-21.

Cha HLJ, Li H, Lee JS, Belova GI, Bulavin DV, Fornace Jr AJ. (2010). Wip1 directly dephosphorylates gamma-H2AX and attenuates the DNA damage response. *Cancer Res* 70: 4112–4222.

Chen GI, Tisayakorn S, Jorgensen C, D'Ambrosio LM, Goudreault M, Gingras AC. (2008) PP4R4/KIAA1622 forms a novel stable cytosolic complex with phosphoprotein phosphatase 4. *J Biol Chem.* 283(43):29273-84.

Chini CC, Wood J, Chen J. (2006). Chk1 is required to maintain claspin stability. *Oncogene.* Jul 13;25(30):4165-71.

Chowdhury D, Keogh MC, Ishii H, Peterson CL, Buratowski S, Lieberman J. (2005). gamma-H2AX dephosphorylation by protein phosphatase 2A facilitates DNA double-strand break repair. *Mol Cell.* 20(5):801-9.

Chowdhury D, Xu X, Zhong X, Ahmed F, Zhong J, Liao J, et al. (2008) A PP4-phosphatase complex dephosphorylates gamma-H2AX generated during DNA replication. *Mol Cell* 31(1):33-46.

Cohen PT, Philp A, Vázquez-Martin C. (2005) Protein phosphatase 4- from obscurity to vital functions. *FEBS Lett.* 579(15):3278-8

da Cruz e Silva OB, da Cruz e Silva EF, Cohen PT (1988). Identification of a novel protein phosphatase catalytic subunit by cDNA cloning. *FEBS Lett.* Dec 19;242(1):106-10.

Dainiak N. (1997) Mechanisms of radiation injury: impact of molecular medicine. *Stem Cells.* 15. Suppl 2:1-5.

Daniel JA, Pellegrini M, Lee JH, Paull TT, Feigenbaum L, Nussenzweig A. (2008) Multiple autophosphorylation sites are dispensable for murine ATM activation in vivo. *J Cell Biol.* 183(5):777-83.

Deininger MW, Bose S, Gora-Tybor J, Yan XH, Goldman JM, Melo JV. (1998) Selective induction of leukemia-associated fusion genes by high-dose ionizing radiation. *Cancer Res.* 58(3):421-5.

DiBiase, S. J., Guan, J., Curran, W. J. Jr., and Iliakis, G. (1999) Repair of DNA double- strand breaks and radiosensitivity to killing in an isogenic group of p53 mutant cell lines. *Int. J. Radiat. Oncol. Biol. Phys.* 45, 743.–751.

Drechsler M, Hildebrandt B, Kundgen A, Germing U, Royer-Pokora B. (2007). Fusion of H4/D10S170 to PDGFRbeta in a patient with chronic

myelomonocytic leukemia and long-term responsiveness to imatinib. *Ann Hematol* 86: 353.–354.

Douglas P, Zhong J, Ye R, Moorhead GB, Xu X, Lees-Miller SP. (2010) Protein phosphatase 6 interacts with the DNA-dependent protein kinase catalytic subunit and dephosphorylates gamma-H2AX. *Mol Cell Biol.* 30(6):1368-81.

Ewing RM, Chu P, Elisma F, Li H, Taylor P, Climie S (2007). Large-scale mapping of human protein-protein interactions by mass spectrometry. *Mol Syst Biol.* 3:89.

Fernandez-Capetillo O, Lee A, Nussenzweig M, Nussenzweig A. (2004) H2AX: the histone guardian of the genome. *DNA Repair (Amst).* 3(8-9):959-67.

Freeman AK, Monteiro AN. (2010) Phosphatases in the cellular response to DNA damage. *Cell Commun Signal.* 8:27.

Fusco A, Grieco M, Santoro M, Berlingieri MT, Pilotti S, Pierotti MA, et al, (1987). A new oncogene in human thyroid papillary carcinomas and their lymph-nodal metastases. *Nature* 328, 170-2.

Gandhi M, Evdokimova V, Nikiforov YE (2010). Mechanisms of chromosomal rearrangements in solid tumours: the model of papillary thyroid carcinoma *Mol Cell Endocrinol* 321(1):36-43.

Gingras AC, Caballero M, Zarske M, Sanchez A, Hazbun TR, Fields S, et al. (2005) A novel, evolutionarily conserved protein phosphatase complex involved in cisplatin sensitivity. *Mol Cell Proteomics.* 4(11):1725-40.

Glatter T, Wepf A, Aebersold R, Gstaiger M. (2009) An integrated workflow for charting the human interaction proteome: insights into the PP2A system. *Molecular Systems Biology* 5:237.

Grieco M, Santoro M, Berlingieri MT, Melillo RM, Donghi R, Borganzone I, et al (1990) PTC is a novel rearranged form of the ret proto-oncogene and is frequently detected in vivo in human thyroid papillary carcinomas. *Cell* 60: 557-563.

Grieco M, Cerrato A, Santoro M, Fusco A, Melillo RM and Vecchio G. (1994). Cloning and characterization of H4 (D10S170), a gene involved in RET rearrangements in vivo. *Oncogene* 9: 2531-5.

Hanada K, Budzowska M, Davies SL, van Drunen E, Onizawa H, Beverloo HB, et al. (2007). The structure-specific endonuclease Mus81 contributes to replication restart by generating double-strand DNA breaks. *Nature Struct Mol Biol* 14: 1096-104.

Harper JW, Elledge SJ. (2007). The DNA damage response: ten years after. *Mol Cell*. 28(5):739-45.

Helps NR, Brewis ND, Lineruth K, Davis T, Kaiser K, Cohen PT (1998). Protein phosphatase 4 is an essential enzyme required for organisation of microtubules at centrosomes in *Drosophila* embryos. *J Cell Sci*. May;111 (Pt 10):1331-40.

Heideker J, Lis ET, Romesberg FE. (2007). Phosphatases, DNA damage checkpoints and checkpoint deactivation. *Cell Cycle* 6: 3058–3064.

Hoeijmakers JH. (2001) Genome maintenance mechanisms for preventing cancer. *Nature*. 411(6835):366-74.

Iurato MP, Scollo C, Belfiore A, Pellegriti G, Salice P, Pezzino V, Giuffrida D, (2000). Differentiated carcinoma of the thyroid in the young. Clinical and histopathologic aspects. *Minerva Endocrinol*. Jun;25(2):39-45.

Jhiang SM. (2000). The RET proto-oncogene in human cancers. *Oncogene*. 19:5590-7.

Jossart G.H, O'Brien B, Cheng J.F, Tong Q, Jhiang S.M, Duh Q, et al. (1996) A novel multicolor hybridization scheme applied to localization of a transcribed sequence (D10S170/H4) and deletion mapping in the thyroid cancer cell line TPC-1. *Cytogenetics and Cell Genetics*, 75:254-257.

Kastan MB, Bartek J (2004) Cell-cycle checkpoints and cancer. *Nature* 432(7015):316-2.

Keogh MC, Kim JA, Downey M, Fillingham J, Chowdhury D, Harrison JC, et al. (2006) A phosphatase complex that dephosphorylates gamma H2AX regulates DNA damage checkpoint recovery. *Nature*. 439(7075):497-501.

Kulkarni S, Heath C, Parker S, Vhase A, Iqbal, Pocock C.F, et al. (2000) Fusion of H4/D10S170 to the platelet-derived growth factor receptor beta in BCR-ABL-negative myeloproliferative disorders with a t(5;10)(q33;q21). *Cancer Research*. 60: 3592-3598.

Kumagai A, Dunphy WG. Claspin, (2000). A novel protein required for the activation of Chk1 during a DNA replication checkpoint response in *Xenopus* egg extracts. *Mol Cell*. Oct;6(4):839-49.

Lazzaro F, Giannattasio M, Puddu F, Granata M, Pelliccioli A, Plevani P, et al. (2009) Checkpoint mechanisms at the intersection between DNA damage and repair. *DNA Repair (Amst)* 8(9):1055- 67.

Lee JH, Paull TT. (2005) ATM activation by DNA double-strand breaks through the Mre11-Rad50-Nbs1 complex *Science* 308(5721):551-4.

Lee DH, Pan Y, Kanner S, Sung P, Borowiec JA, Chowdhury D. (2010). A PP4 phosphatase complex dephosphorylates RPA2 to facilitate DNA repair via homologous recombination. *Nat Struct Mol Biol* 17: 365–372.

Lee SJ, Lim CJ, Min JK, Lee JK, Kim YM, Lee JY et al. (2007). Protein phosphatase 1 nuclear targeting subunit is a hypoxia inducible gene: its role in post-translational modification of p53 and MDM2. *Cell Death Differ* 14: 1106–1116.

Lu G, Wang YB. (2008). Functional diversity of mammalian Type 2C protein phosphatase isoforms: New tales from an old family. *Clin Exp Pharm Physiol* 35: 107–112.

Lupas A, Van Dyke M, Stock J. (2009). Predicting coiled coils from protein sequences. *Science*. 1991 May 24;252:1162-4.

Leone V, Mansueto G, Pierantoni GM, Tornincasa M, Merolla F, Cerrato A, et al (2010) CCDC6 represses CREB1 activity by recruiting histone deacetylase 1 and protein phosphatase 1. *Oncogene*. 29(30):4341-51.

Macurek L, Lindqvist A, Voets O, Kool J, Vos HR, Medema RH. (2010) Wip1 phosphatase is associated with chromatin and dephosphorylates gammaH2AX to promote checkpoint inhibition. *Oncogene*. 29(15):2281-91.

Merolla F, Pentimalli F, Pacelli R, Vecchio G, Fusco A, Grieco M et al. (2007) Involvement of H4(D10S170) protein in ATM-dependent response to DNA damage. *Oncogene*. 26(42):6167-75.

Moon SH, Lin L, Zhang X, Nguyen TA, Darlington Y, Waldman AS et al. (2010). Wildtype p53-induced phosphatase 1 dephosphorylates histone variant {gamma}-H2AX and suppresses double strand break repair. *J Biol Chem* 285: 12935–12947.

Motoyama N, Naka K. (2004). DNA damage tumor suppressor genes and genomic instability. *Curr Opin Genet Dev* 14: 11–16.

Mohammad DH, Yaffe MB, (2009). 14-3-3 proteins, FHA domains and BRCT domains in the DNA damage response. *DNA Repair (Amst)*. Sep 2;8(9):1009-17. Epub May 29. Review.

Mihindikulasuriya KA, Zhou G, Qin J, Tan TH, (2004). Protein phosphatase 4 interacts with and down-regulates insulin receptor substrate 4 following tumor necrosis factor-alpha stimulation. *J Biol Chem*. Nov 5;279(45):46588-94.

Nakada S, Chen GI, Gingras AC, Durocher D (2008). PP4 is a gamma H2AX phosphatase required for recovery from the DNA damage checkpoint. *EMBO Rep*. 9(10):1019-2

Nikiforova MN, Stringer JR, Blough R., Medvedovic M., Fagin JA and Nikiforov YE, (2000). Proximity of chromosomal loci that participate in radiation-induced rearrangements in human cells. *Science* 290:138-41.

Nikiforov YE. (2006) Radiation-induced thyroid cancer: what we have learned from Chernobyl. *Endocr Pathol*. 17, 307-317.

Nikiforov YE, Nikiforova MN, (2011). Molecular genetics and diagnosis of thyroid cancer. *Nat Rev Endocrinol*. Aug 30;7(10):569-80. doi: 10.1038/nrendo.2011.142.

Norbury CJ, Zhivotovsky B. DNA damage-induced apoptosis. *Oncogene*. 2004 Apr 12;23(16):2797-808. Review.

O'Neill BM, Szyjka SJ, Lis ET, Bailey AO, Yates JR 3rd, Aparicio OM, et al. (2007). Pph3-Psy2 is a phosphatase complex required for Rad53 dephosphorylation and replication fork restart during recovery from DNA damage. *Proc Natl Acad Sci U S A*. 104(22):9290-9295.

Ostrowski ML, Merino MJ, (1996). Tall cell variant of papillary thyroid carcinoma: a reassessment and immunohistochemical study with comparison to the usual type of papillary carcinoma of the thyroid. *Am J Surg Pathol* 20(8):964-74.

Peng A, Lewellyn AL, Schiemann WP, Maller JL. (2010). Repo-man controls a protein phosphatase 1-dependent threshold for DNA damage checkpoint activation. *Curr Biol* 20: 387–396.

Pierotti MA, Santoro M, Jenkins RB, Sozzi G, Bongarzone I, Grieco M, (1992) Characterization of an inversion on the long arm of chromosome 10 juxtaposing D10S170 and RET and creating the oncogenic sequence RET/PTC. *Proc Natl Acad Sci* 89:1616-20.

Puxeddu E, Knauf JA, Sartor MA, Mitsutake N, Smith EP, Medvedovic M, et al. (2005). RET/PTC-induced gene expression in thyroid PCCL3 cells reveals early activation of genes involved in regulation of the immune response. *Endocr Relat Cancer*. 12(2):319-3.

Reinhardt HC, Yaffe MB. (2009). Kinases that control the cell cycle in response to DNA damage: Chk1, Chk2, and MK2. *Curr Opin Cell Biol*. (2):245-55

Rogakou EP, Pilch DR, Orr AH, Ivanova VS, Bonner WM (1998). DNA double-stranded breaks induce histone H2AX phosphorylation on serine 139. *J Biol Chem* 273: 5858.–5868.

Ron E, Lubin JH, Shore RE, Mabuchi K, Modan B, Pottern LM, et al, (1995). On target cell numbers in radiation-induced H4-RET mediated papillary thyroid. cancer. *Radiat Res* 141(3):259-77.

Salvatore G, De Falco V, Salerno P, Nappi TC, Pepe S, Troncone G, Carlomagno F, Melillo RM, Wilhelm SM, Santoro M., (2006). BRAF is a therapeutic target in aggressive thyroid carcinoma. *Clin Cancer Res*. Mar 1;12(5):1623-9.

Santoro M, Chiappetta G, Cerrato A, Salvatore D, Zhang L, Manzo G, et al, (1996). Development of thyroid papillary carcinomas secondary to tis-

sue-specific expression of the RET/PTC1 oncogene in transgenic mice. *Oncogene* 12(8):1821-6.

Shiloh Y. (2003). ATM and related protein kinases: safeguarding genome integrity. *Nat Rev Cancer*. 3(3):155-6.

Speit, G. and Hartmann, A. (1995) The contribution of excision repair to the DNA-effects seen in the alkaline single cell gel test (comet assay). *Mutagenesis* 10, 555.–559.

Schwaller J, Anastasiadou E, Cain D, Kutok J, Wojiski S, Williams IR, et al (2001). H4(D10S170), a gene frequently rearranged in papillary thyroid carcinoma, is fused to the platelet-derived growth factor receptor beta gene in atypical chronic myeloid leukemia with t(5;10)(q33;q22). *Blood*. 97(12):3910-3918.

Takahashi M, Buma Y, Iwamoto T, Inaguma Y, Ikeda H, Hiai H, (1988). Cloning and expression of the ret proto-oncogene encoding a tyrosine kinase with two potential transmembrane domains. *Oncogene* 3(5):571-8.

Tsai IC, Hsieh YJ, Lyu PC, Yu JS. (2005). Anti-phosphopeptide antibody, P-STM as a novel tool for detecting mitotic phosphoproteins: identification of lamins A and C as two major targets. *J Cell Biochem* 94(5):967-81.

Tong Q, Li Y, Smanik PA, Fithian LJ, Xing S, Mazzaferri EL, Jhiang SM, (1995) Characterization of the promoter region and oligomerization domain of H4 (D10S170), a gene frequently rearranged with the ret proto-oncogene. *Oncogene* 10(9):1781-7.

Tong, Q, Xing S and Jhiang SM, (1997). Leucine zipper-mediated dimerization is essential for the PTC1 oncogenic activity. *J Biol Chem* 272:9043-7.

Tung HY, Alemany S, Cohen P. (1985). The protein phosphatases involved in cellular regulation. Purification, subunit structure and properties of protein phosphatases-2A0, 2A1, and 2A2 from rabbit skeletal muscle. *Eur J Biochem.* 148(2):253-63.

Virshup DM, Shenolikar S. (2009). From Promiscuity to Precision: Protein Phosphatases Get a Makeover. *Mol Cell* 33: 537–545.

Wang B, Zhao A, Sun L, Zhong X, Zhong J, Wang H, et al. (2008) Protein phosphatase PP4 is overexpressed in human breast and lung tumours. *Cell Res.* 18(9):974-7.

Ward JF. (1995). Radiation mutagenesis: the initial DNA lesions responsible. *Radiat Res*, 142(3):362-8.

Williams ED. (1977). The epidemiology of thyroid cancer. *Ann Radiol (Paris)* 20(8):722-4.

Williams D. (2002). Cancer after nuclear fallout: lessons from the Chernobyl accident. *Nat Rev Cancer* 2(7):543-9. Review.

Zhang X, Ozawa Y, Lee H, Wen YD, Tan TH, Wadzinski BE, Seto E. (2005). Histone deacetylase 3 (HDAC3) activity is regulated by interaction with protein serine/threonine phosphatase 4. *Genes Dev* 19(7):827-39.

Zhou BB, Elledge SJ. (2000). The DNA damage response: putting checkpoints in perspective. *Nature*. 408(6811):433-9.

Zhou G, Mihindikulasuriya KA, MacCorkle-Chosnek RA, Van Hooser A, Hu MC, Brinkley BR, Tan TH, (2002). Protein phosphatase 4 is involved in tumor necrosis factor-alpha-induced activation of c-Jun N-terminal kinase. *J Biol Chem*. 277(8):6391-8

Zhou G, Boomer JS, Tan TH. (2004). Protein phosphatase 4 is a positive regulator of hematopoietic progenitor kinase 1. *J Biol Chem*. 279(47):49551-61

LIST OF PUBLICATIONS

A. **Francesco Merolla, Chiara Luise, Tony Sourisseau, Spiros Liaropoulos, Roberto Pacelli, Alfredo Fusco and Angela Celetti.** CCDC6 is a stress response protein that preserves genome stability upon interaction with PP4c. *Oncogene*, re-submitted after revision.

B. **Chiara Luise, Francesco Merolla, Vincenza Leone, Alfredo Fusco and Angela Celetti.** Identification of sumoylation sites in CCDC6, the first identified RET partner gene, uncover a mode of regulating CCDC6 function on CREB1 transcriptional activity. *European Journal of Endocrinology*, submitted.

C. **Chiara Luise, Francesco Merolla, Maria Siano, Enza Leone, Genaro Ilardi, Paolo Chieffi, Alfredo Fusco, Stefania Staibano and Angela Celetti.** "CCDC6: a new DNA damage response mediator in cancer", *British Journal of Cancer*, submitted.

D. **Angela Celetti, Francesco Merolla, Chiara Luise, Maria Siano, Stefania Staibano.** Book Title: "Intraepithelial Neoplasia", Chapter Title: Novel markers for oral intraepithelial neoplasia. InTech Editor, ISBN 978-953-307-764-2, in press.